Archivum Immunologiae et Therapiae Experimentalis
74, 4 (2026), DOI: 10.2478/aite-2026-0004

ORIGINAL

Immune Surveillance in Chronic Myeloid Leukemia: Tumor Antigen Expression and CD8$^+$ T Cell Function in the Context of Treatment-Free Remission

Paulina Kwaśnik[1] · Martyna Stępień[1] · Katarzyna Skórka[1] · Magdalena Paziewska[1] · Agnieszka Karczmarczyk[1] · Michalina Pinkosz[1] · Paweł Cech[1] · Joanna Zaleska[1] · Michał Kiełbus[1,2] · Dorota Link-Lenczowska[3] · Magdalena Zawada[3] · Tomasz Sacha[4,#] · Krzysztof Giannopoulos[1]✉[#]

Abstract

This study evaluated the immune surveillance function in chronic myeloid leukemia (CML) through tumor antigen gene expression analysis, *in vitro* mixed lymphocyte cultures with peptides, and immunological analysis of patients after imatinib withdrawal to investigate factors affecting treatment-free remission (TFR). Specific immune responses were demonstrated in T lymphocytes against SPAG9 and NY-REN-60 peptides, highlighting their potential in immunotherapy. Immune profiling identified that CD8$^+$PD1$^+$, CD56^{dim}CD16$^+$PD1$^+$, and iNKT$^+$CD161$^+$ cells contribute to recurrence-free survival. A Cox model confirmed the prognostic value of immune markers. These results emphasize the critical role of the immune system in CML and indicate novel targets for sustaining TFR.

Keywords
Chronic myeloid leukemia • Treatment-free remission • Imatinib discontinuation • Peptide vaccines • Immune biomarker

Received: 15 May 2025 / Accepted: 16 September 2025 /
© L. Hirszfeld Institute of Immunology and Experimental Therapy, Wrocław, Poland 2025

Abbreviations

CI, confidence intervals; CML, chronic myeloid leukemia; CTL, cytotoxic T lymphocytes; DC, dendritic cells; DMR, deep molecular response; ELTS, EUTOS long-term survival (score); EUTOS, European treatment and outcome study (score); HLA-A2, human leukocyte antigen A2; HR, hazard ratios; LAA, leukemia-associated antigen; LSCs, leukemic stem cell(s); MHC, major histocompatibility complex; MLPC, mixed lymphocyte peptide culture; MMR, major molecular response; NK, natural killer cells; NKT, natural killer T cells; iNKT, invariant natural killer T cells; PBMC, peripheral blood mononuclear cells; PBS, phosphate-buffered saline; TFR, treatment-free remission; TKI, tyrosine kinase inhibitor; TREG, regulatory T lymphocytes.

1. Introduction

Immune dysfunction and immunosurveillance in chronic myeloid leukemia (CML) have long been an unmet need for clarification, especially in the context of treatment-free remission (TFR) achieved only by a subset of patients (Mahon et al. 2010; Ross et al. 2013; Mori et al. 2015; Nicolini et al. 2018; Saussele et al. 2018). Historical evidence from the era before the introduction of tyrosine kinase inhibitors (TKI), including the curative potential of allogeneic stem cell transplantation (alloSCT), has indicated that CML is a disease susceptible to immune-mediated control (van Rhee et al. 1994; Kolb et al. 1995; Collins et al. 1997; Sehn et al. 1999; Guglielmi et al. 2002; Huff et al. 2006; Maurer and Antin 2024). Beyond their direct effects on BCR::ABL1 tyrosine kinase, TKI are now also recognized for their immunomodulatory properties (Tanaka et al. 2020; Vigón et al. 2020). At diagnosis, CML patients demonstrate an impaired immune response, involving natural killer (NK) cells, dendritic cells (DC), and cytotoxic T lymphocytes (CTL), manifested by a reduction in their number and function (Braga et al. 2024). Furthermore, CTL directed against CML cells exhibit high expression of PD1 (programmed death receptor 1), which, upon binding to PD1 ligand (PDL1) expressed on CML cells, leads to inhibition of the cell-killing capacity of these cells and, consequently, disease progression (Mumprecht et al. 2009). Patients diagnosed with CML also have a high percentage of regulatory T lymphocytes (Treg), which are suppressor immune cells that promote T cell dysfunction, thus contributing to tumor cell escape from immune surveillance (Giallongo et al. 2014; Hughes et al. 2017; Najima et al. 2018). Immunological

[#] *These authors contributed equally to this work.*

[1] *Department of Experimental Hematooncology, Medical University of Lublin, Lublin, Poland*
[2] *Department of Biochemistry and Molecular Biology, Medical University of Lublin, Lublin, Poland*
[3] *Diagnostic Department of Hematology and Genetics, The University Hospital in Kraków, Kraków, Poland*
[4] *Department of Hematology, Jagiellonian University Medical College in Kraków, Kraków, Poland*

✉ *krzysztof.giannopoulos@gmail.com*

parameters improve during TKI therapy. In patients treated with TKI, an expansion of $CD8^+$ CTL and NK cells is observed, which is associated with a better response to treatment (Mustjoki et al. 2009; Chang et al. 2019; Kreutzman et al. 2019). Moreover, interferon-α (IFN-α) treatment has been observed to stimulate the immune system, and combination therapies of imatinib and IFN-α improve treatment outcomes (Ross et al. 2013; Saussele et al. 2018). This immunomodulatory effect may influence the achievement of deep molecular response (DMR) and, therefore, the possibility of achieving TFR despite fluctuations in *BCR::ABL1* levels. Studies suggest that DMR is associated with an increased percentage of cytotoxic cells and a decreased number of suppressor cells, suggesting the involvement of immunocompetent cells in immune surveillance, which is important for achieving long-term remission without treatment (Hughes et al. 2017; Ilander et al. 2017; Cayssials et al. 2019; Irani et al. 2020; Fujioka et al. 2021; Kong et al. 2021; Kwaśnik and Giannopoulos 2021). Patients achieving durable TFR are characterized by elevated numbers and cytotoxic activity of NK cells ($CD56^{dim}CD16^+$, increased interferon-γ (IFN-γ) production, and expression of activating receptors), as well as the presence of antigen-specific $CD8^+$ clones (e.g. anti-PR1), and innate $CD8^+$ T cells (Rea et al. 2017; Cayssials et al. 2019; Kong et al. 2021; Decroos et al. 2024; Garcia et al. 2024; Huuhtanen et al. 2024). In turn, increased PD1 expression on T lymphocytes is associated with unfavorable TFR outcomes (Hughes et al. 2017; Decroos et al. 2024; Garcia et al. 2024; Kwaśnik et al. 2024). These findings highlight the potential of immune surveillance mechanisms in maintaining TFR.

Immune characterization in CML is relevant to new immunotherapies that target enhancing the patient's immune system through leukemia-associated antigen (LAA) vaccines that hold promise for $CD8^+$ cytotoxic T cell responses and increased CTL expansion, or combination therapies that include IFN-α or immune checkpoints as a response enhancer to improve TFR rates (Liu et al. 2024).

In this study, we analyzed the expression of characterized tumor-associated gens in CML patients at diagnosis (n = 43). Additionally, we conducted a comprehensive evaluation of the immune system in patients with sustained TFR (n = 78) and investigated effector immune responses in a subset of post-imatinib patients (n = 3).

2. Materials and Methods

2.1. Patient samples

Tumor antigen expression was assessed in peripheral blood samples collected at diagnosis from 43 patients with newly diagnosed CML, as part of routine diagnostic procedures at collaborating centers. Clinical data were unavailable due to anonymization of samples at the time of referral. The study group included 22 women (51%) and 21 men (49%) with a median age of 66 years (age range: 30–92 years).

A group of 78 patients with CML who achieved a DMR of at least MR4.0 were included in the imatinib discontinuation trial and analyzed for maintenance of TFR. Samples were collected at particular time points after imatinib withdrawal: at the moment of discontinuation and 3 months, 6 months, 9 months, and 12 months of TFR. Four patients could obtain a sample at a longer time interval after treatment discontinuation. Of the study participants, 58% (45/78) were women and 42% (33/78) were men, with a median age of 64 years (age range, 25–87 years).

Additionally, three CML patients (two men aged 76 years and 44 years, and one woman aged 56 years) at the time of imatinib discontinuation underwent functional tests using the Enzyme-Linked ImmunoSpot (ELISpot) assay. At the moment of treatment discontinuation, all patients were in DMR. In patient p114, the quantity of *BCR::ABL1* transcript was detected at 0.0014, corresponding to an MR4.5 response, while no transcript was detected in patients p122 and p129, classifying the molecular response at MR5.0. The amount of *BCR::ABL1* transcript was assessed by droplet digital PCR (ddPCR). One of the three analyzed patients experienced a molecular recurrence, defined as loss of major molecular response (MMR) already at 3 months after imatinib withdrawal, while the other two patients remained in remission. The length of imatinib treatment before discontinuation was 54 months in patient no. 114, 66 months in patient no. 122 and 73.5 months in patient no. 129. The duration of DMR before imatinib discontinuation was 46 months in patient p114, 57 months in patient p122, and 55 months in patient p129, respectively.

The study received approval from the Ethics Committee of the Medical University of Lublin (approval number KE-0254/174/2017) and was conducted in accordance with the Declaration of Helsinki. Written informed consent was obtained from all participants.

2.2. Cell isolation

Peripheral blood mononuclear cells (PBMCs) were isolated with density gradient centrifugation using Biocoll (Biochrom, Berlin, Germany). The viability of the cells, anticipated to be above 95%, was assessed using trypan blue staining (Sigma Aldrich, Saint Louis, MO, USA). Cells were cryopreserved in medium consisting of RPMI 1640 (Biochrom), fetal bovine serum (FBS, Biochrom), and dimethyl sulfoxide (DMSO, Sigma Aldrich) in a 7:2:1 ratio, respectively.

2.3. RNA isolation

RNA was isolated using the QIAamp RNA Blood Mini Kit (Qiagen) according to the manufacturer's protocol. The concentration and purity of the extracted RNA samples

were assessed using a BioSpec-nano spectrophotometer (Shimadzu, Kyoto, Japan). The RNA samples were stored at –80°C for further analysis.

2.4. Reverse transcription reaction

The reverse transcription reaction was performed using the QuantiTect Reverse Transcription Kit (Qiagen), following the manufacturer's instructions. For each sample, 1 µg of RNA was reverse-transcribed to 20 µL of cDNA.

2.5. Assessment of gene expression using quantitative PCR (qPCR)

To evaluate the *HMMR* (encode RHAMM, hyaluronan-mediated motility receptor), *WT1* (WT1, Wilm's tumor 1), *PRTN3* (PR3, proteinase 3), *AURKA* (AURKA, aurora kinase A), *DNAJC2* (MPP11, M-phase phosphoprotein 11 protein), *USP32* (NY-REN-60, renal cell carcinoma associated antigen 60), *SPAG9* (SPAG9, sperm-associated antigen 9), and *PRAME* (PRAME, preferentially expressed antigen in melanoma) mRNA expression levels, qPCR was performed using the TaqMan Real-Time PCR analysis kit (Applied Biosystem (Thermo Fisher Scientific, Waltham, MA, USA) according to the manufacturer's instructions and the 7500 Fast Dx Real-Time PCR Instrument (Applied Biosystems). As a reference gene, the constitutive gene *GAPDH* (glyceraldehyde–3–phosphate dehydrogenase) was used. For each reaction, 1 µL of the cDNA sample was used as a template for qPCR analysis. Additionally, a negative control (NC) was performed, in which 1 µL of distilled water was added. Gene expression levels were expressed as ΔCt values, calculated as the difference between the ΔCt of the target gene and the ΔCt of the *GAPDH* reference gene.

2.6. Quantification of *BCR::ABL1* transcripts by ddPCR

The ddPCR test was performed according to the described procedure (Kjaer et al. 2019). Molecular recurrence is confirmed loss of MMR, assessed on two occasions, 1 month apart.

2.7. Flow cytometry for detection of immune populations

Flow cytometric analysis was performed on PBMC collected at the time of treatment discontinuation (0 month) and during the TFR trial at subsequent time points: 3 months, 6 months, and 12 months. One million PBMC were incubated for 20 min at room temperature (RT) in the dark with fluorochrome-labeled monoclonal antibodies (mAb) (all from BD Biosciences, San Jose, CA, USA).

Immunophenotypic analysis included B cells ($CD19^+$) and T cells ($CD3^+$): $CD8^+$ T cells (including the $CD8^+PD1^+$ subpopulation), and $CD4^+$ T cells (including the Treg subpopulation, and the $CD4^+PD1^+$ subpopulation), using the following mAb: anti-CD3-BV510, anti-CD4-PerCP, anti-CD8-FITC, anti-CD19-APC-Cy7, anti-CD25-PE-Cy7, and anti-CD127-BV421. Treg were identified using the Human FOXP3 Fix/Perm Buffer Set (Becton Dickinson, San Jose, CA, USA) and intracellular staining with anti-FOXP3-PE for 30 min at RT, according to the manufacturer's protocol. A minimum of 100,000 stained cells per sample was acquired.

NK and natural killer T (NKT) cell populations were analyzed using the following mAb: anti-CD45-BV510, anti-CD14-APC-H7, anti-CD3-PerCP, anti-CD56-PE-Cy7, anti-CD16-BV421, anti-iNKT-FITC, and anti-CD161-PE. A minimum of 100,000 stained cells per sample was acquired.

Conventional DC and plasmacytoid DC were assessed using the following mAb panel: anti-CD3, CD14, CD19, CD20, CD56-FITC (antibody cocktail), anti-HLA-DR-BV510, anti-CD123-PE-Cy7, anti-BDCA-1-PE, anti-BDCA-BV421. A minimum of 300,000 events were collected per sample.

Anti-PD1-APC was used to evaluate PD1 expression on B, T, NK, and DC cell subsets.

Anti-HLA serotype A*0201-FITC was used to identify HLA-A2 positive patients.

Before analysis, cells were washed twice with PBS or stain buffer (for Treg staining). Fluorescence minus one (FMO) controls were used to define gating thresholds for PD1 and FOXP3 expression. All samples were acquired using a FACSLyric flow cytometer (Becton Dickinson) and analyzed with FACS Suite software (version 1.5, Becton Dickinson).

2.8. Prediction of amino residue sequences of the MHC I epitope derived from SPAG9 and NY-REN-60 peptides restricted to HLA-A*0201

The binding affinity of MHC class I-restricted epitopes derived from SPAG9 and NY-REN-60 to HLA serotype A*0201 molecules was calculated using three independent computer prediction algorithms: Synthetic Peptide Homologous to T-cell Epitopes and its Interactions (SYFPEITHI) (Rammensee et al. 1999), the Immune Epitope Database (IEDB) (Vita et al. 2019), and NetCTL algorithm (version 1.2; Technical University of Denmark) (Larsen et al. 2007). In the SYFPEITHI and NetCTL algorithms, the number of assigned points is proportional to the binding affinity of the peptide to the HLA-A*0201 molecule, while for the IEDB algorithm, it is inversely proportional.

Twelve peptides from SPAG9 and twelve peptides from NY-REN-60, selected based on their highest-ranking positions predicted by the algorithms, were selected (Table 1).

All peptides were synthesized by JPT Peptide Technologies (Berlin, Germany). The purity of the peptides was at least

74, 4 (2026), DOI: 10.2478/aite-2026-0004

Table 1. *SPAG9 and NY-REN-60 derived T cell epitope peptides predicted by computer algorithms SYFPEITHI, IEDB, and NetCTL*

Peptide	Peptide sequence	Peptide position	SYFPEITHI ranking	IEDB ranking	NetCTL ranking
S1	SLLGGITVV	837	32	0.4	1.27
S2	ALADGTLAI	1016	29	0.7	1.42
S3	AIIESTPEL	343	29	1.6	1.30
S4	ELMPLVVAV	49	28	0.4	1.03
S5	VMSERVSGL	19	26	1.6	1.21
S6	RLMELQEAV	521	25	0.3	1.20
S7	SLFEELSSA	381	25	1.0	1.19
S8	KLKDSILSI	998	26	2.3	1.34
S9	VLQGELEAV	447	28	1.7	1.02
S10	AVLENLDSV	56	26	1.8	1.07
S11	LILENTQLL	413	26	3.0	1.08
S12	DLIAKVDEL	433	28	5.6	-
N1	WLLSGGVYV	162	26	0.4	1.26
N2	SLFGMPLIV	1099	26	0.5	1.23
N3	FMNSSIQCV	744	24	0.4	1.49
N4	SLSEGLFNA	231	24	0.5	1.26
N5	FLVPRDPAL	1311	25	0.9	1.33
N6	LLFQVCHIV	355	24	0.43	1.23
N7	LLAFLLDGL	829	29	1.3	1.08
N8	GLHEDLNRV	836	28	1.3	1.10
N9	LLDDEDHKL	679	26	2.0	1.60
N10	NLIVGLVLL	79	30	1.6	0.93
N11	FLCAFEIPV	991	22	0.1	1.37
N12	MMRTELYFL	1083	23	0.9	1.24

IEDB, immune epitope database; SYFPEITHI, Synthetic Peptide Homologous to T-cell Epitopes and its Interactions.

95%, as determined by high-performance liquid chromatography (HPLC). All peptides were diluted in DMSO and PCR-grade clean water under sterile conditions.

2.9. The T2 peptide-binding assay and culture of the cell line

The T2 peptide-binding assay was performed to evaluate the ability of *in silico*-predicted peptides to bind the HLA-A*0201 molecule *in vitro*. The T2 cell line was obtained from the DSMZ-German Collection of Microorganisms and Cell Cultures GmbH (Braunschweig, Germany) and cultured in RPMI 1640 medium (Biochrom) supplemented with 10% FBS (Biochrom) and 1% antibiotics (Penicilin-Streptomycin-Neomycin Solution Stabilized, Sigma Aldrich).

T2 cells (4×10^6/one peptide) were pulsed with a series of seven concentrations of peptides (range 0.5–50 µg/mL) or with 1 µL of DMSO as a NC, supplemented with 5 µg/mL beta-2 microglobulin (Sigma Aldrich) and incubated for 18 h in 5% CO_2 at 37°C. Afterwards, cells were washed and incubated with fluorochrome-labeled monoclonal antibody anti-HLA-A2 FITC for 15 min at RT in the dark, then washed twice with PBS. Cells were analyzed using a FACSLyric (Becton Dickinson) and FACS Suite software (version 1.5, Becton Dickinson). The fluorescence intensity (FI) factor was calculated as the ratio of the mean fluorescence intensity (MFI) of HLA-A*0201 on T2 cells with peptide to the MFI of HLA-A*0201 on T2 cells without peptide, using the formula FI = MFI (T2 with peptide)/MFI (T2 without peptide) (Gross et al. 2004).

2.10. Mixed lymphocyte peptide culture

Mixed lymphocyte peptide culture (MLPC) was used to determine the immunogenicity of synthesized peptides in an *in vitro* model of the immune response.

$CD8^+$ cells from HLA-A*0201-positive CML patients were separated using CD8 magnetic microbeads (Miltenyi Biotec, Bergisch Gladbach, Germany) and MS magnetic-activated cell sorting (MACS) columns (Miltenyi Biotec) according to the manufacturer's instructions. CD8- cells, representing antigen-presenting cells (APC), were irradiated with 25 Gy

and incubated for 2 h with 20 µg/mL of the respective peptide derived from (I) NY-REN-60 (N11, FLCAFEIPV), and (II) SPAG9 (S4, ELMPLVVAV), (III) a mixture of peptides derived from RHAMM-R3$_{165–173}$, WT1$_{126–134}$, PRAME$_{300–309}$, MPP11$_{437–445}$, Aur-A$_{207–215}$, BCR-ABL$_{922–930}$, and PR3-PR1$_{169–177}$ (10 µg/mL of each peptide), (IV) without any peptide as a NC. The sequences of the peptides used in the peptide mixture are shown in Table 2. Afterwards, CD8$^-$ cells were mixed with CD8$^+$ cells in a 4:1 ratio and incubated in CTL Test Medium (CTL, Cleveland, OH, USA), supplemented with 10% FBS and 1% antibiotics in 5% CO_2 at 37°C. After an overnight incubation, the cells were stimulated with 2.5 ng/mL human interleukin (IL)-2 (Sigma Aldrich) and 20 ng/mL recombinant human IL-7 (Sigma Aldrich). Cells were restimulated with IL-2, and IL-7 was added every 3 days.

After 7 days, the cells were restimulated by freshly irradiated CD8$^-$ cells incubated with the respective peptides in the same order and concentrations as described above, and half of the medium was changed. After 14 days, specific IFN-γ and granzyme B release from CD8$^+$ cells was assessed in an ELISpot assay (Diaclone, Besançon, France).

2.11. Specific IFN-γ and granzyme B release

Assessment of specific IFN-γ and granzyme B release was performed using Human IFN-γ/Granzyme B Dual ELISpot according to the manufacturer's protocol (Diaclone).

First, 96-well polyvinylidene fluoride (PVDF) bottomed plates were treated with 35% ethanol and coated with anti-IFN-γ and anti-granzyme B capture antibodies. After overnight incubation at 4°C, the plates were washed with PBS. Afterwards, the blocking buffer, consisting of liquid milk and PBS in a 1:1 ratio, was added to each well in triplicate and incubated for 2 h at RT. Simultaneously, T2 cells were pulsed for 2 h at 37°C with respective peptides derived from (I) NY-REN-60 (N11, FLCAFEIPV) and (II) SPAG-9 (S4, ELMPLVVAV), or (III) mixture of peptides: RHAMM-R3$_{165–173}$, WT1$_{126–134}$, PRAME$_{300–309}$, MPP11$_{437–445}$, Aur-A$_{207–215}$, BCR-ABL$_{922–930}$, and PR3-PR1$_{169–177}$, (IV) without any peptide as a NC (in the same order as CD8- cells were pulsed), or (V) with the non-specific positive control, Pokeweed Mitogen (PWM, Sigma Aldrich). Plates were washed with PBS, then CD8$^+$ T cells (1 × 10^4) and T2 cells (4 × 10^4) were added to each well in triplicate and incubated for 15–20 h in 5% CO_2 at 37°C. After incubation, plates were washed with 0.05% Tween-PBS Solution (Tween 20, Bio-Rad, Hercules, CA, USA). Next, the detection antibodies were added to each well and incubated for 1.5 h at RT. The plates were then washed with 0.05% Tween PBS Solution, after which streptavidin-alkaline phosphatase (AP) and anti-FITC anti-Horseradish Peroxidase (HRP) conjugates were added to each well and incubated for 1 h at RT. The plates were then washed with 0.05% Tween-PBS Solution, then 3-amino-9-ethylcarbazole (AEC) and BCIP/NBT (5-bromo-4-chloro-3-indolyl phosphate/nitroblue tetrazolium) buffers were added to each well to visualize the presence of colored spots. Cells producing IFN-γ appeared as red or brownish spots, while those producing granzyme B appeared as blue or purple spots. Results were evaluated using an ImmunoSpot ELISPOT reader (CTL, Shaker Heights, OH, USA).

Table 2. *Sequences of peptides used in the peptide mix in the MLPC*

Peptide	Peptide sequence
RHAMM-R3$_{165–173}$	ILSLELMKL
WT1$_{126–134}$	RMFPNAPYL
PRAME$_{300–309}$	ALYVDSLFFL
MPP11$_{437–445}$	STLCQVEPV
Aur-A$_{207–215}$	YLILEYAPL
BCR-ABL$_{922–930}$	GFKQSSKAL
PR3-PR1$_{169–177}$	VLQELNVTV

MLPC, mixed lymphocyte peptide culture.

2.12. Statistical analysis

Statistical analysis and data visualization were performed using R software, version 4.1.3 (R Foundation for Statistical Computing, Vienna, Austria) and GraphPad Prism 8 software (GraphPad Software, San Diego, CA, USA). A *p*-value <0.05 was considered statistically significant. Where applicable, *p*-values were adjusted for multiple comparisons using the Benjamini-Hochberg procedure to maintain a false discovery rate of 5% (Benjamini and Hochberg 1995). Confidence intervals (CI) were calculated at the 95% level. For comparisons of continuous or ordinal variables between two independent patient subgroups, the Mann–Whitney *U* test was utilized. For comparisons involving more than two independent subgroups, the Kruskal–Wallis test was applied. The survival analysis included data from 69 patients. To investigate the association between immune cell populations and recurrence risk, a Cox proportional hazards model was developed using the survival package in R. This approach was chosen to model time-to-recurrence, with outcomes and model predictions considered at specific follow-up intervals (0 month, 3 months, 6 months, 9 months, and 12 months). The mathematical formulation of the Cox proportional hazards model is expressed as:

$$h(t) = h_0(t) \cdot e\beta 1X1 + \beta 2X2 + \beta 3X3 + \ldots + \beta nXn$$

where $h(t)$ is the hazard function, $h_0(t)$ is the baseline hazard function, X_i are the covariates, and $beta_i$ are their respective coefficients.

For the development of the multivariable Cox model, predictors were selected using a bidirectional stepwise procedure guided by the Akaike information criterion (AIC). The AIC informed the selection process by balancing the model's log-likelihood against the number of included parameters, thereby penalizing excessive complexity. The objective of this iterative procedure was to derive a parsimonious model with optimal predictive utility while minimizing the risk of overfitting. The final model incorporated iNKT^{+}CD161^{+}, CD8^{+}PD1^{+}, and CD56^{dim}16^{+}PD1^{+} as predictors. The model's performance was evaluated by examining hazard ratios (HRs) with their 95% CI, *p*-values for individual predictors, and the Concordance Index (C-index) for overall discriminative ability. The proportional hazards assumption, critical for the validity of the Cox model, was verified using Schoenfeld residual tests. Furthermore, Pearson correlation analysis among the selected predictors revealed weak correlations ($|r| < 0.15$), indicating minimal multicollinearity and suggesting that each variable contributed independent information. To assess the stability of the variable selection process and the robustness of the final model, bootstrap resampling (100 iterations) was employed. This validation step focused on the consistency of variable inclusion and the variability of the AIC, aiming to ensure the model's generalizability and minimize the risk of overfitting. Forest plots, generated using the ggforest function within the survminer package in R, were utilized to visualize the HR and 95% CI for the predictors in the final model.

3. Results

3.1. Screening of *HMMR*, *WT1*, *PRTN3*, *AURKA, DNAJC2*, *USP32, SPAG9*, and *PRAME* gene expression in CML patients

The study screened the expression of genes encoding the analyzed tumor antigens. Expression of the *HMMR* (Me = 94.51), *PRTN3* (Me = 752.53), *AURKA* (Me = 56.11), and *DNAJC2* (Me = 55.32) genes was demonstrated in all analyzed patients. *SPAG9* gene expression (Me = 51.10) was shown in 97.67% (42/43) of patients, *WT1* (Me = 26.79), and *USP32* (Me = 55.99) gene expression was shown in 95.35% (41/43) of the CML patients, while *PRAME* gene expression (Me = 65.43) was shown in 90.70% (39/43) of the patients.
The results of the Kruskal–Wallis test showed statistically significant differences between the analyzed genes ($p < 0.0001$). The Mann–Whitney test showed statistically significantly higher gene expression of the following genes (Figure 1):

- *HMMR* compared to *WT1* (94.51 *vs*. 26.79; $p = 0.02$),
- *PRTN3* compared to *HMMR* (752.50 *vs*. 94.51; $p < 0.01$),
- *PRTN3* compared to *WT1* (752.50 *vs*. 26.79; $p < 0.0001$),
- *AURKA* compared to *WT1* (56.11 *vs*. 26.79; $p = 0.01$),
- *DNAJC2* compared to *WT1* (55.32 *vs*. 26.79; $p = 0.03$),
- *USP32* compared to *WT1* (55.99 *vs*. 26.79; $p = 0.04$),
- *SPAG9* compared to *WT1* (51.10 *vs*. 26.79; $p = 0.03$),
- *PRTN3* compared to *AURKA* (752.50 *vs*. 56.11; $p < 0.0001$),
- *PRTN3* compared to *DNAJC2* (752.50 *vs*. 55.32; $p < 0.0001$),
- *PRTN3* compared to *USP32* (752.50 *vs*. 55.99; $p < 0.0001$),
- *PRTN3* compared to *SPAG9* (752.50 *vs*. 51.10; $p < 0.0001$),
- *PRTN3* compared to *PRAME* (752.50 *vs*. 65.43; $p < 0.01$).

No statistically significant differences in expression were shown between the other pairs of genes.

3.2. Evaluation of the correlation of *HMMR*, *WT1*, *PRTN3*, *AURKA*, *DNAJC2*, *USP32*, *SPAG9* and *PRAME* gene expression in CML patients

Spearman correlation was used to assess the correlation of expression between the analyzed genes (Figure 2). Very strong positive correlations were shown between *HMMR* and *USP32* ($r = 0.93$, $p < 0.0001$, Figure 2a), and *USP32* and *SPAG9* ($r = 0.93$; $p < 0.0001$, Figure 2b). Moreover, there were strong positive correlations between *HMMR* and *PRTN3* ($r = 0.69$; $p < 0.0001$, Figure 2c), *HMMR* and *AURKA* ($r = 0.62$; $p < 0.0001$, Figure 2d), *PRTN3* and *AURKA* ($r = 0.69$; $p < 0.0001$, Figure 2e), and *AURKA* and *DNAJC2* ($r = 0.64$, $p < 0.0001$, Figure 2f). In addition, moderate positive correlations were observed between *HMMR* and *WT1* ($r = 0.44$, $p < 0.01$, Figure 2g), *AURKA* and *USP32* ($r = 0.49$, $p = 0.001$, Figure 2h), *AURKA* and *SPAG9* ($r = 0.55$; $p < 0.001$, Figure 2i), *DNAJC2* and *USP32* ($r = 0.54$; $p < 0.001$, Figure 2j) and *DNAJC2* and *SPAG9* ($r = 0.54$; $p < 0.001$, Figure 2k). A weak positive correlation was also noted between *WT1* and *PRTN3* ($r = 0.35$; $p = 0.03$, Figure 2l). Among the remaining genes, correlations were not statistically significant.

3.3. Evaluation of the correlation between *HMMR*, *WT1*, *PRTN3*, *AURKA*, *DNAJC2*, *USP32*, *SPAG9* and *PRAME* gene expression and the clinical parameters of CML patients

An assessment of the correlation between the expression of the *HMMR*, *WT1*, *PRTN3*, *AURKA*, *DNAJC2*, *USP32*, *SPAG9*, and *PRAME* genes, and CML patients' age and gender was performed. No statistically significant correlation was found between the expression of any of the analyzed genes and either age (Table 1 in Supplementary Materials) and gender (Figure 1 in Supplementary Materials).

3.4. Affinity for in silico-designed peptides derived from SPAG9 and NY-REN-60 antigens

Based on the obtained results, the peptide S4 was selected from the SPAG9 antigen, and the N11 peptide from the NY-REN-60 antigen, characterized by the highest intensity

74, 4 (2026), DOI: 10.2478/aite-2026-0004

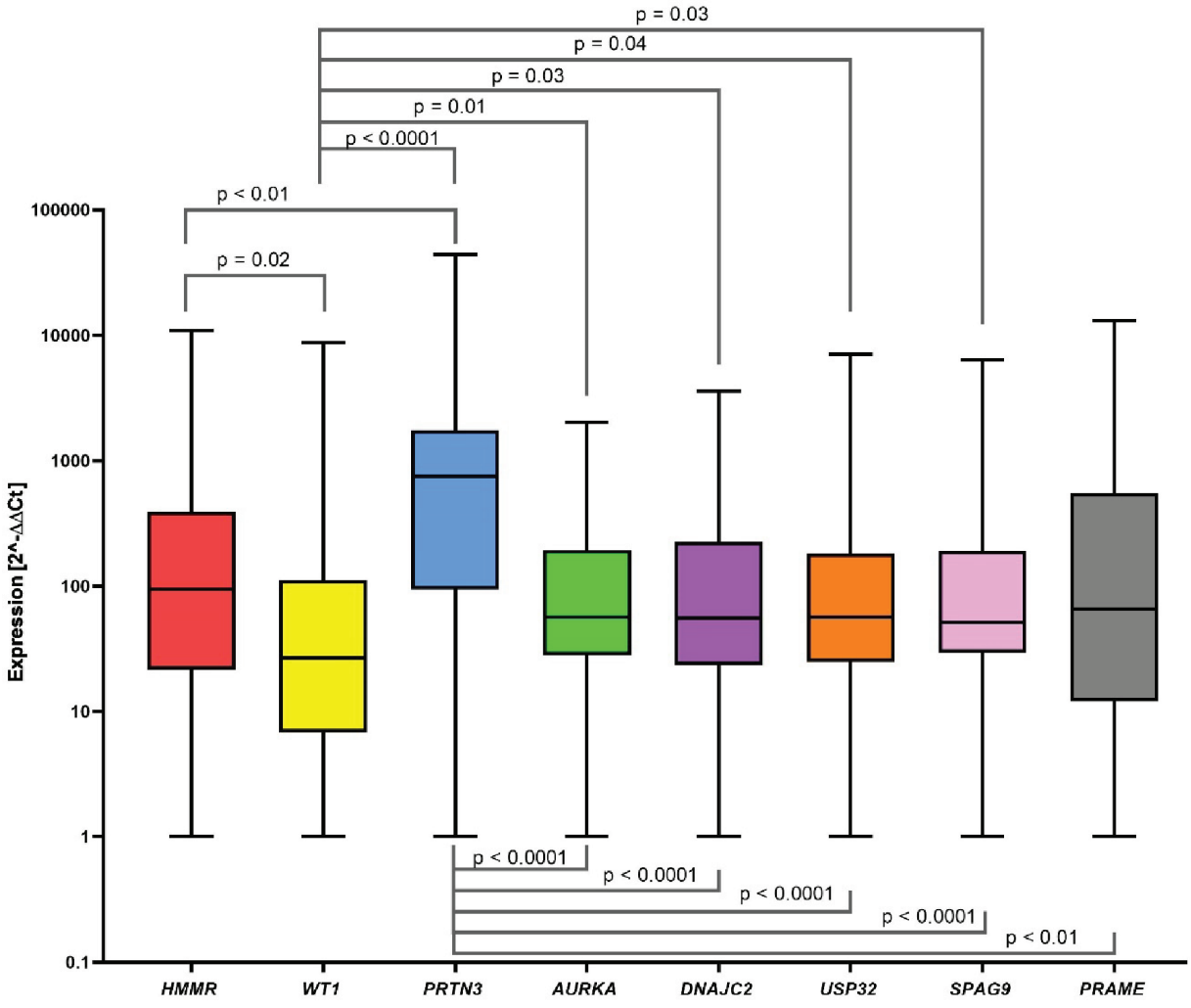

Fig 1. *Screening of HMMR, WT1, PRTN3, AURKA, DNAJC2, USP32, SPAG9, and PRAME gene expression in CML patients. The data is presented in a box and a whisker plot, where the whiskers indicate the min-max value, and the box marks the median. We observed statistically significant higher gene expression of HMMR vs. WT1, AURKA vs. WT1, DNAJC2 vs. WT1, USP32 vs. WT1, SPAG9 vs. WT1, PRTN3 vs. HMMR, WT1, AURKA, DNAJC2, USP32, SPAG9, and PRAME. In the remaining pairs, no statistical significance was obtained. CML, chronic myeloid leukemia.*

of receptor fluorescence compared to the NC (Figure 3). The ELISpot functional test was performed to assess whether the selected peptides trigger an immune response of T lymphocytes.

3.5. Evaluation of specific secretion of IFN-γ and granzyme B by immunoenzymatic lymphocyte activation test

We detected specific cytotoxic immune responses against S4 and N11 peptides derived from SPAG9 and NY-REN-60 antigens, respectively. Furthermore, a specific cytotoxic immune response, defined by granzyme B release, was observed in two out of three patients at the moment of imatinib discontinuation, which was more intense than the mixture of previously known immune-driven peptides with documented efficacy from RHAMM-R3, WT1, PRAME, MPP-11, Aur-A, BCR-ABL, and PR3-PR1 antigens. The granzyme B-mediated response suggests potent cytotoxic antitumor activity of immune cells. Interestingly, the patient in whom no lymphocyte activation was detected as a result of stimulation with peptides derived from tumor antigens had a disease recurrence already at 3 months after imatinib withdrawal, in contrast to the other two patients who remained in remission. In addition, a very weak immune response defined by IFN-γ release was detected, possibly due to the short duration of cell culture.

These results may indicate that SPAG9 and NY-REN-60 allow immune recovery to occur more rapidly during imatinib

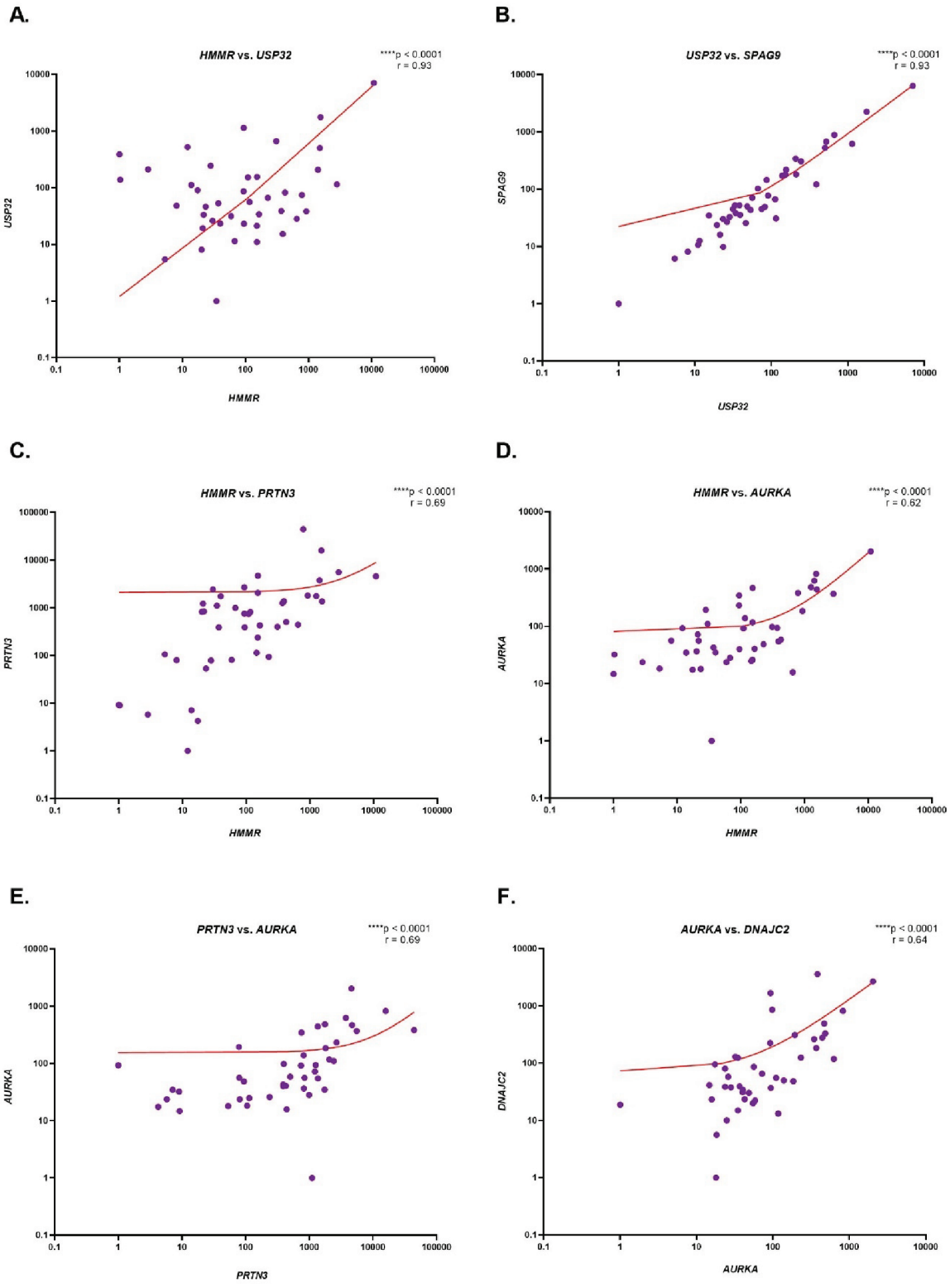
A.
HMMR vs. USP32
****p < 0.0001
r = 0.93
USP32
HMMR
B.
USP32 vs. SPAG9
****p < 0.0001
r = 0.93
SPAG9
USP32
C.
HMMR vs. PRTN3
****p < 0.0001
r = 0.69
PRTN3
HMMR
D.
HMMR vs. AURKA
****p < 0.0001
r = 0.62
AURKA
HMMR
E.
PRTN3 vs. AURKA
****p < 0.0001
r = 0.69
AURKA
PRTN3
F.
AURKA vs. DNAJC2
****p < 0.0001
r = 0.64
DNAJC2
AURKA

(*Continued*)

74, 4 (2026), DOI: 10.2478/aite-2026-0004

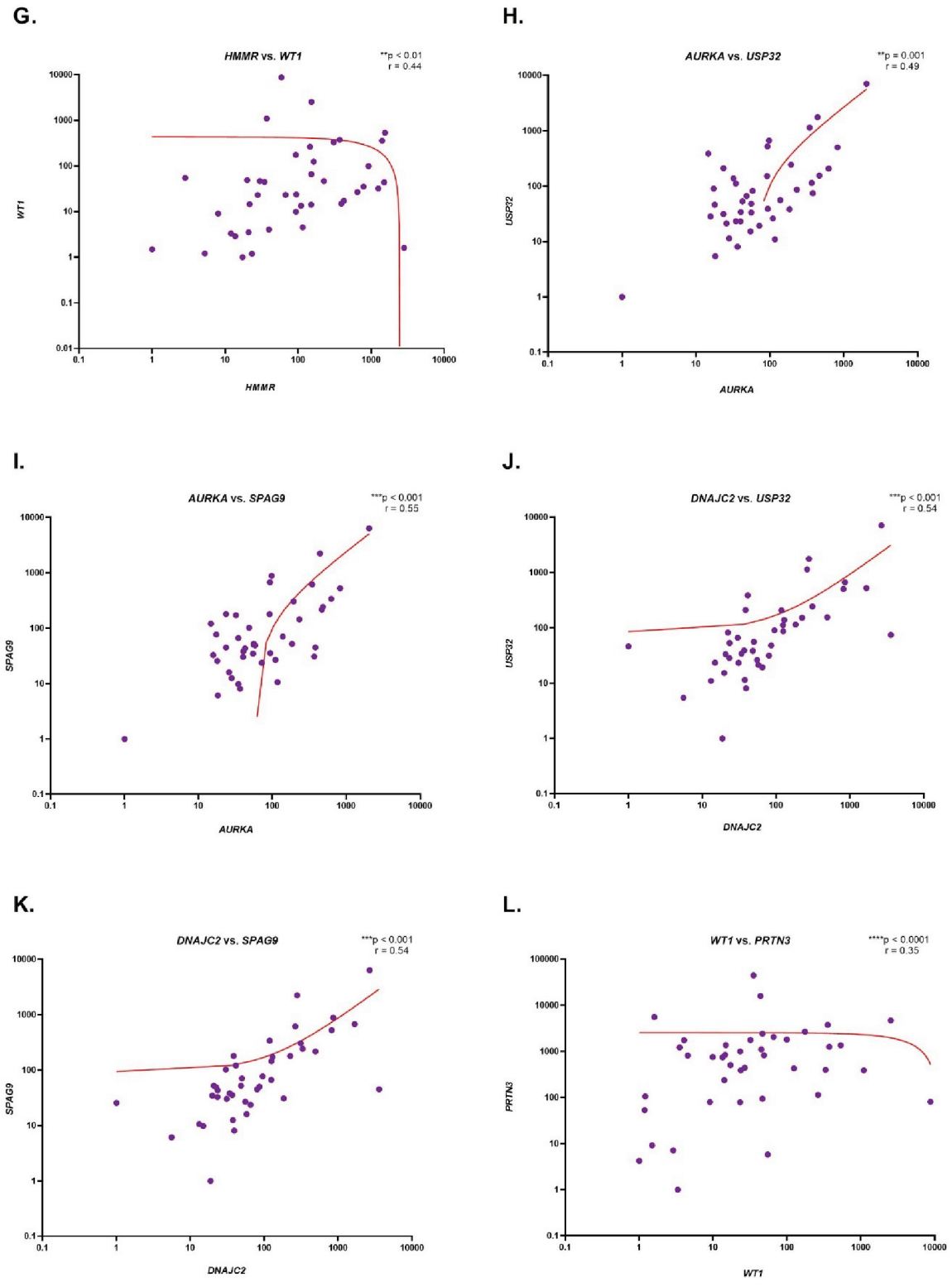

Fig 2. *Evaluation of the correlation of HMMR, WT1, PRTN3, AURKA, DNAJC2, USP32, SPAG9 and PRAME gene expression in CML patients. The results are presented as the log10 value of 2^-ΔΔCt with the regression line marked. The graph shows only statistically significant correlations between HMMR and USP32* ***(A)****, USP32 and SPAG9* ***(B)****, HMMR and PRTN3* ***(C)****, HMMR and AURKA* ***(D)****, PRTN3 and AURKA* ***(E)****, AURKA and DNAJC2* ***(F)****, HMMR and WT1* ***(G)****, AURKA and USP32* ***(H)****, AURKA and SPAG9* ***(I)****, DNAJC2 and USP32* ***(J)****, DNAJC2 and SPAG9* ***(K)****, WT1 and PRTN3* ***(L)****. CML, chronic myeloid leukemia.*

74, 4 (2026), DOI: 10.2478/aite-2026-0004

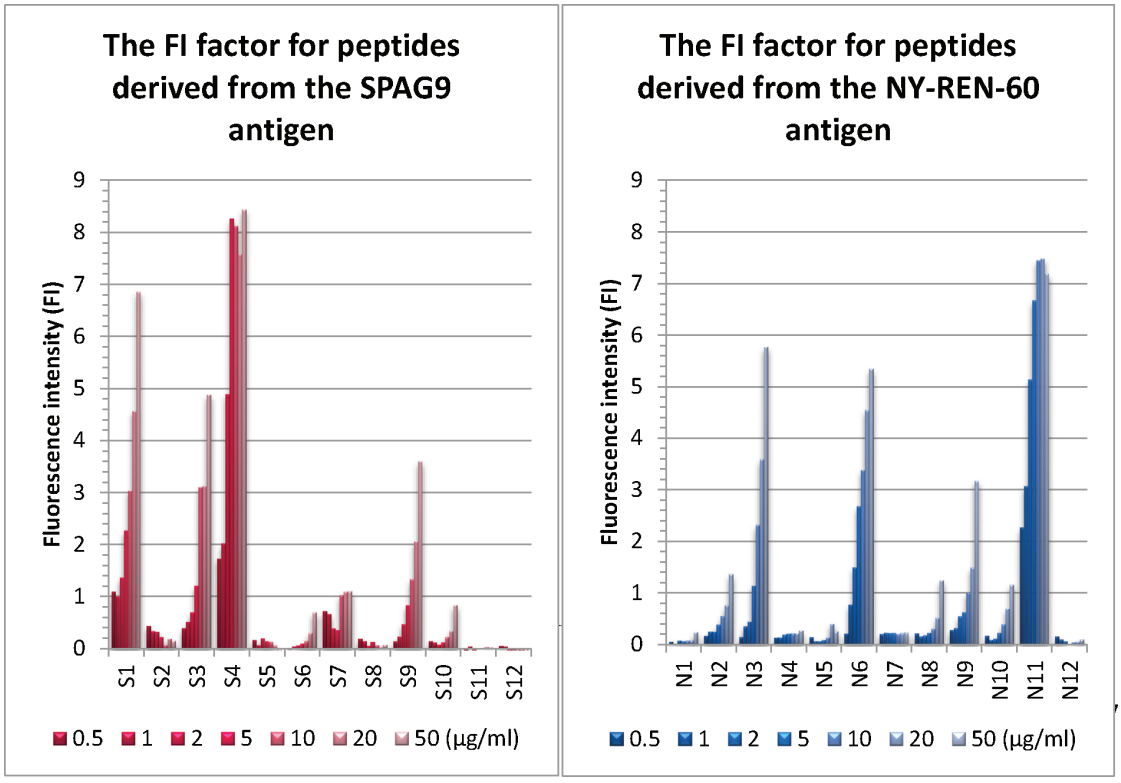

Fig 3. *FI factor for peptides derived from SPAG9 and NY-REN-60 antigens in the T2 peptide-binding assay. The affinity of 12 newly synthesized peptides (from SPAG9: S1–S12; from NY-REN-60: N1-N11) to the HLA-A2 receptor was assessed by adding the peptides at specific concentrations: 0.5 µg/mL, 1 µg/mL, 2 µg/mL, 5 µg/mL, 10 µg/mL, 20 µg/mL, and 50 µg/mL to the T2 cell line using two replicates. The FI factor was calculated as the ratio of the MFI of HLA-A*0201 on T2 cells with peptide to the MFI of HLA-A*0201 on T2 cells without peptide, using the formula FI = MFI (T2 with peptide)/MFI (T2 without peptide). FI, Fluorescence intensity; MFI, mean fluorescence intensity.*

treatment than the standard peptide mixture known so far. Figure 4 shows the results of IFN-γ (red, brownish dots) and granzyme B (blue dots) release by T cells in response to peptide stimulation and a non-specific positive control (PWM). The response to tumor antigens tested as a peptide mix is very weak, which may be due to the lack of expression in these patients or due to imatinib-induced transient recalibration of the immune system, with cytotoxic mechanisms dominating. Since IFN-γ is a marker of Th1-type response and is usually released by helper T cells and some subpopulations of cytotoxic cells, its absence may result from preferential activation of CTL, which are more focused on direct destruction of tumor cells than on IFN-γ secretion. The poor response in terms of IFN-γ release may also be due to too low a concentration of the peptides used in the assay.

The stronger response was described in patient no. 122, and it was characterized by the presence of normal blood morphology, indicative of a healthy state. The p122 noted an increased frequency of DC and a reduced expression of PD1 on both DCs and NK cells compared to p114, characterized by a weak immune response. In addition to the weaker immune response, this patient also had lower levels of $CD8^+$ T cells. The number of regulatory T cells in the relapsed patient (p114) was nearly three times higher than in the patient who remained in remission. This increase may suppress the immune response, promoting the survival of LSC and ultimately leading to disease relapse after treatment discontinuation. The impairment of the immune response in patient p114 may also be related to the depth of the molecular response, which reached the level of MR4.5, while in patients p122 and p129, the *BCR::ABL1* transcript (MR5.0) was not detected at the time of imatinib discontinuation. Moreover, the duration of imatinib treatment and the duration of DMR before the TFR attempt, which was shorter in patient number 114 (54 months and 46 months, respectively) compared to patient number 122 (*vs*. 66 months and 57 months) and 129 (*vs*. 73.5 months and 55 months), may be important factors in the relapse of leukemia (Hughes and Ross 2016).

3.6. Evaluation of the immune system in patients with sustained TFR

The Cox proportional hazards model with time intervals but without time-dependent covariates was used to evaluate the

prognostic value of specific immune cell populations. The model was built using time-split data, where each observation corresponds to a specific time interval (start, stop). The validity of this approach was confirmed by the Schoenfeld residual test, which did not indicate a violation of the proportional hazards assumption ($p > 0.05$ for all covariates). Classical prognostic scores (Sokal, EUTOS, ELTS) were available for a subset of patients only and therefore, were not incorporated into the present Cox regression model. Given that all patients in this cohort had already achieved DMR at the time of TKI discontinuation, our analysis was designed to specifically focus on immune predictors of molecular recurrence. The final multivariate model, developed through a stepwise selection procedure, was specified as follows:

$$h(t)=h_0(t)\exp(-2.36\cdot iNKT^{+}CD161^{+}+0.03\cdot CD8^{+}PD1^{+}0.11\cdot CD56^{dim}CD16^{+}PD1^{+})$$

The results of both the univariate and final multivariate analyses are summarized in Table 3. The multivariate model identified three significant independent predictors of recurrence. A higher percentage of $iNKT^{+}CD161^{+}$ cells was strongly associated with a protective effect (HR = 0.09, $p = 0.001$), while higher levels of both $CD8^{+}PD1^{+}$ cells (HR = 1.03, $p < 0.001$) and $CD56^{dim}CD16^{+}PD1^{+}$ cells (HR = 1.12, $p < 0.001$) were associated with an increased risk.

The table displays the results from both univariate and multivariate Cox proportional hazards models. HRs, 95% CI, and *p*-values are shown for the three predictors included in the final multivariate model. HR < 1 indicates a protective effect, while HR > 1 indicates an increased risk of recurrence. The model, based on 189 observations (64 events), demonstrated good predictive accuracy (C-index = 0.735), with highly significant results in the likelihood ratio test, Wald test, and log-rank test ($p < 10^{-6}$) (Figure 2 in Supplementary Materials).

To further assess the model's clinical relevance, patients were stratified into high-risk and low-risk groups based on the linear predictor (risk score) derived from the Cox model. The median risk score was used as the threshold, classifying patients accordingly. Kaplan–Meier survival analysis showed a clear separation between the two groups, with the high-risk group

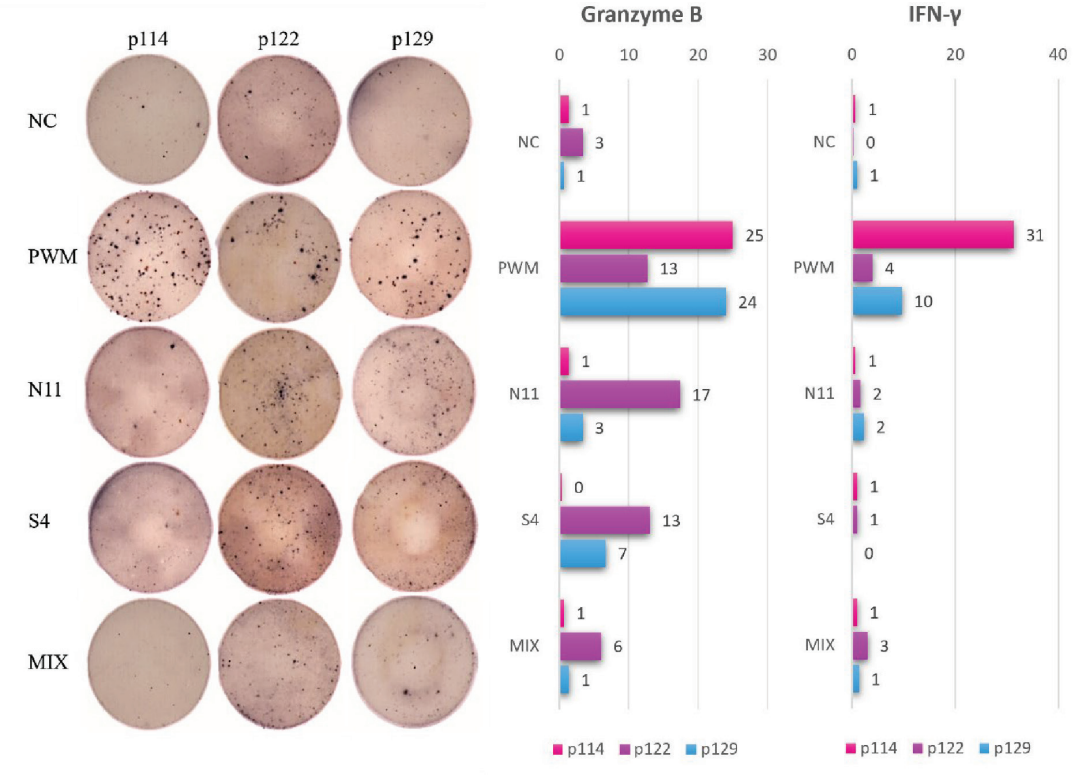

Fig 4. *Results of specific IFN-γ (red, brownish dots) and granzyme B (blue dots) release in response to peptide derived from tumor-associated antigens stimuli. The ELISpot assay was performed after mixed lymphocyte-peptide culture. $CD8^{+}$ cells were pulsed with $CD8^{-}$ cells stimulated by N11 peptide derived from NY-REN-60 antigen and S4 peptide derived from SPAG9 antigen, as well as the mixture of peptides: RHAMM-R3$_{165–173}$, WT1$_{126–134}$, PRAME$_{300–309}$, MPP11$_{437–445}$, Aur-A$_{207–215}$, BCR-ABL$_{922–930}$, and PR3-PR1$_{169–177}$. NC was $CD8^{+}$ CML cells cultured without any peptide; PWM as a non-specific control was added to NC cells on ELISpot plates. IFN-γ and granzyme B spots were obtained from 10^{4} cytotoxic T cells per well and spot averages were calculated from triplets. CML, chronic myeloid leukemia; ELISpot, Enzyme-Linked ImmunoSpot; IFN-γ, interferon-γ; NC, negative control; PWM, pokeweed mitogen.*

Table 3. *Univariate and multivariate Cox proportional hazards analysis of immune cell populations for recurrence risk*

Variable	Univariate analysis		Multivariate analysis	
	HR (95% CI)	*p*-value	HR (95% CI)	*p*-value
iNKT^{+}CD161^{+}	0.32 (0.11–0.94)	0.039	0.09 (0.02–0.40)	0.001
CD8^{+}PD1^{+}	1.03 (1.02–1.05)	<0.001	1.03 (1.02–1.05)	<0.001
CD56^{dim}CD16^{+}PD1^{+}	1.06 (1.01–1.11)	0.024	1.12 (1.05–1.19)	<0.001

CI, confidence interval; HR, hazard ratio.

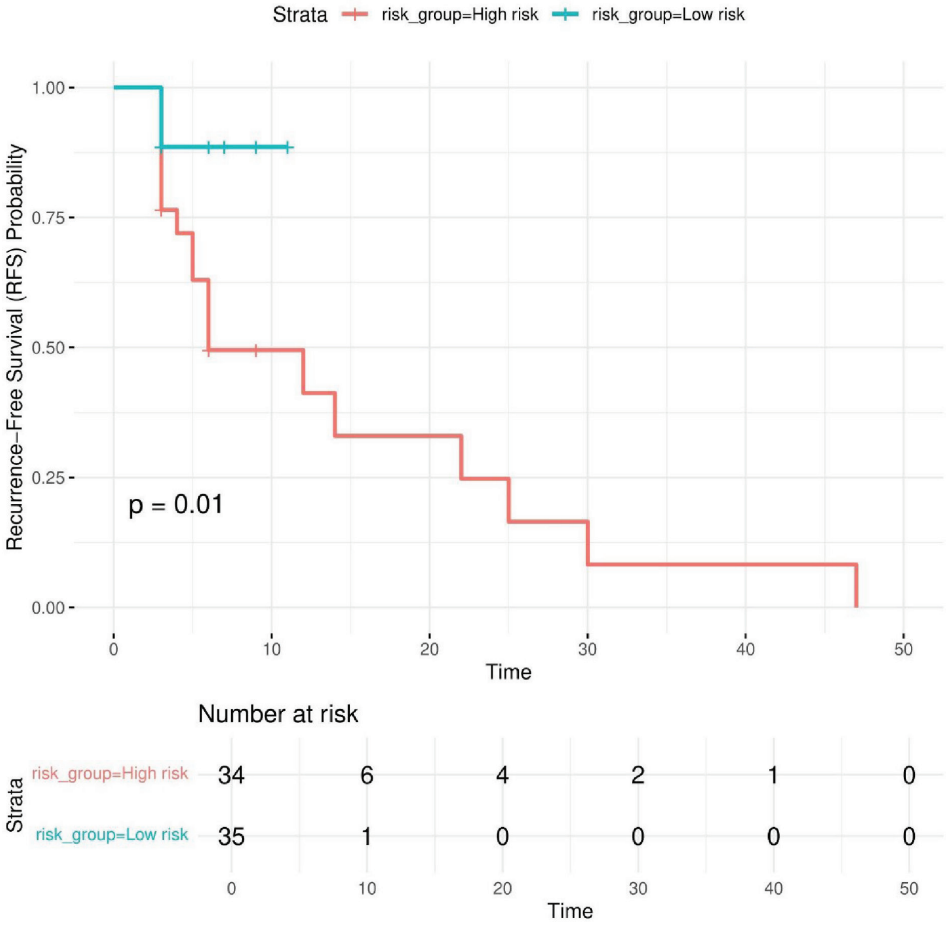

Fig 5. *Kaplan–Meier survival curves for high-risk and low-risk patient groups. The Kaplan–Meier plot illustrates RFS in patients stratified into high-risk and low-risk groups based on the median risk score derived from the Cox proportional hazards model and appropriately colored. The survival curves show a clear separation between the two groups, with the high-risk group exhibiting significantly worse RFS, while the low-risk group demonstrates longer recurrence-free intervals. The p-value ($p < 0.05$) indicates that the difference between the groups is statistically significant, confirming the model's ability to distinguish between different risk categories. RFS, recurrence-free survival.*

exhibiting significantly worse recurrence-free survival (Figure 5). Conversely, patients in the low-risk group demonstrated longer recurrence-free intervals, reinforcing the protective role of iNKT^{+}CD161^{+} and the potential negative impact of CD8^{+}PD1^{+} and CD56^{dim}CD16^{+}PD1^{+}. The observed differences were statistically significant ($p < 0.05$), confirming the model's ability to effectively differentiate between risk categories.

To assess the stability and generalizability of the model, we performed non-parametric bootstrap validation with 100 resampling iterations. The bootstrap analysis yielded the following results: Original AIC = 436.375, indicating the model's relative goodness-of-fit, Bias = 1.212, suggesting minimal overfitting, and Standard error = 43.152, reflecting variability in AIC across bootstrap samples. These results confirm that

the model remains robust across different resampled datasets, with only minor variation in performance metrics. The low bias indicates that the model's estimates are stable, and the observed variability in AIC suggests that the model retains predictive value despite potential dataset fluctuations. The full results of both univariate and multivariate Cox regression analyses are summarized in Tables 2 and 3 in Supplementary Materials, respectively.

These findings demonstrate that the Cox model effectively identifies immune markers associated with recurrence risk. The results suggest that iNKT^{+}CD161^{+} may have a protective role, while CD8^{+}PD1^{+} and CD56^{dim}CD16^{+}PD1^{+} cells are linked to an increased hazard, indicating their potential contribution to poorer outcomes. Bootstrap validation confirms the model's robustness, showing minimal overfitting and consistent predictive performance. Overall, these results underscore the potential of immune profiling as a valuable tool for patient stratification and recurrence risk assessment in clinical practice.

Importantly, the identified associations are biologically plausible: higher frequencies of iNKT^{+}CD161^{+} cells may contribute to effective immune surveillance and elimination of residual leukemic clones, whereas elevated CD8^{+}PD1^{+} T cells and PD1^{+} NK cells are consistent with an exhausted phenotype associated with impaired cytotoxic function and a higher risk of molecular relapse.

4. Discussion

The immune system is thought to be crucially implicated in the control of CML, but it is uncertain to what extent the endogenous immune response maintains control of CML during TKI therapy in the chronic phase or after discontinuation of TKI administration. This study aimed to investigate the expression of tumor genes to characterize CML patients at diagnosis. Besides, we followed the immune responses in 78 CML patients who discontinued imatinib therapy, additionally assessing effector mechanisms of CTL in three patients with DMR that could influence extended remission or relapse using the MLPC in an *in vitro* model of the immune response. Our results provide evidence of tumor antigen presentation in newly diagnosed CML patients and suggest that cytotoxic immune responses may be associated with long-term remission after discontinuation of TKI. However, we emphasize that our observations are associations, not establishing a causal relationship between immune activity and leukemia control.

Expression of the *HMMR, WT1, PRTN3, AURKA, DNAJC2, USP32, SPAG9*, and *PRAME* genes was detected in more than 90% of patient samples. Strong positive correlations existed between *HMMR* and *USP32*, and between *USP32* and *SPAG9*, suggesting a potential co-regulatory process that would be associated with modulating leukemic cell survival and immune recognition. Interestingly, the strong expression and correlation between the *USP32* gene, which encodes NY-REN-60, and *SPAG9*, which encodes SPAG9, may potentially reflect the anticancer vaccine value of such antigens, considering the particular immune response of CD8^{+} lymphocytes against *in silico*-designed peptides N11 of NY-REN-60 and S4 of SPAG9 that we identified in functional studies. While previous studies have documented the immunogenicity of these antigens in solid tumors (Greiner and Schmitt 2008; Kanojia et al. 2010; Šmahel 2011; Li et al. 2012, 2024; Hu et al. 2017; Pan et al. 2018; Dou et al. 2020; Xiu et al. 2023), their role in hematological malignancies, including CML, remains to be further elucidated.

The previous studies indicate that tumor antigen expression is implicated in immune-mediated regulation of leukemia (Clark and Christmas 2001; Clark et al. 2001; Rezvani et al. 2003; Giannopoulos et al. 2009). The identification of these antigens is valuable to provide a glimpse into antigenic targets that have the potential to be useful for future immunotherapeutic treatments in CML, based on peptide vaccines or antibody-drug conjugates, as well as for specific immunotherapies aimed at enhancing the graft-versus-leukemia effect after alloSCT (Greiner and Schmitt 2008). Initial clinical trials demonstrated that vaccination with BCR::ABL1 peptides could induce a leukemia-specific T cell response and transient reductions in *BCR::ABL1* transcript levels (Cathcart et al. 2004; Bocchia et al. 2005; Rojas et al. 2007; Abruzzese et al. 2009). However, the depth and durability of molecular responses were limited, highlighting the challenges of early peptide-based vaccination approaches. Importantly, recent long-term data have reshaped this perspective. The two multicenter phase II trials with 10-year follow-up (Sicuranza et al. 2025) demonstrated that BCR::ABL1 (e14a2- and e13a2-derived peptides) peptide vaccination during TKI therapy is safe, devoid of off-target toxicity, and capable of sustaining TFR, suggesting that peptide-based immunotherapy in CML deserves renewed clinical consideration. WT1, another well-characterized LAA, was also shown in case reports to elicit peptide-specific cytotoxic T-cell responses in patients with myeloid malignancies, including CML, although clinical effects were modest and often transient (Narita et al. 2010; Oji et al. 2010; Takahashi 2015). However, vaccines directed against WT1 combined with PR1 or PRAME may further improve targeting of leukemic cells, increasing response rates (Rezvani et al. 2008; Yong et al. 2008). This suggests that multiantigen strategies may overcome the limitations of single-antigen vaccines by inducing sustained long-term antileukemic responses. More recently, studies highlight that WT1 peptide vaccination can elicit deep molecular remissions and lasting CTL responses that persisted 12 years after vaccination cessation (Suwabe et al. 2024). Furthermore, clinical trials using PR1 peptide vaccines have induced

specific CTL responses that correlate with clinical responses, including in patients with CML (Qazilbash et al. 2017). These findings provide a translational bridge between our immune profiling results and future vaccine-based therapeutic strategies aimed at enhancing TFR. The synergistic effect of vaccination with conventional TKI therapy may further reduce residual disease and, in TKI-resistant patients, may improve treatment outcomes, but further studies on the relationship between vaccination and patients' clinical responses are warranted. In contrast, a randomized phase II trial comparing the K562/GM-CSF cell-based vaccine with IFN-α used in combination with a TKI showed that vaccinated individuals had lower TFR rates than the IFN-α group, highlighting the potential benefit of IFN-α therapy in combination (Webster et al. 2021). However, the ENDURE CML-IX trial did not demonstrate an improvement in TFR rates after initiating IFN-α therapy after TKI treatment discontinuation (Burchert et al. 2022). The impact of maintaining IFN-α therapy on TFR when patients receive a combination of TKIs and IFNs before discontinuing TKI therapy may prove crucial. On the other hand, it is possible that enhancing the Th1 immune response alone may not be sufficient for long-term disease control. Studies of checkpoint immunotherapy have shown modest clinical benefit. Preclinical studies have shown that blocking the PD1/PDL1 interaction prolongs survival in a mouse model of CML (Mumprecht et al. 2009). However, in a phase 1b clinical trial, the combination of dasatinib with nivolumab failed to demonstrate significant clinical activity in patients with refractory or progressive CML (Martínez-López et al. 2021). A current phase II trial is underway, combining pembrolizumab (anti-PD1) with various TKIs (dasatinib, imatinib, nilotinib) in patients with persistent minimal residual disease (ClinicalTrials.gov: NCT03516279). These findings underscore the complexity of immune evasion in CML and suggest that enhancing immune recognition may not be sufficient to eliminate leukemic stem cells. Our findings add to the growing evidence that tumor antigen expression can modulate immune responses in leukemia, but further studies are required to establish their utility as targets for treatment. Functional studies showed peptide-specific cytotoxic T-cell responses against SPAG9 and NY-REN-60 antigens. The granzyme B release observed in two patients upon discontinuation of imatinib treatment suggests a functional cytotoxic response, potentially contributing to leukemia control. In contrast, the patient with relapse (p114) showed a lack of T-cell activation, which coincided with subsequent molecular relapse, suggesting that impaired immune responses may be associated with leukemia relapse. This patient's immune profile, characterized by an increased percentage of Treg and elevated PD1 expression on DC and NK cells, reflects a depleted immune phenotype that potentially impairs leukemia surveillance. These observations are consistent with previous studies describing immune dysfunction in patients with relapsed CML (Rea et al. 2017; Fujioka et al. 2021; Kong et al. 2021).

Our Cox regression model identified significant immune markers for the risk of recurrence. The protective role of iNKT^{+}CD161^{+} cells and the detrimental effect of CD8^{+}PD1^{+} and CD56^{dim}CD16^{+}PD1^{+} cells suggest that some immune subsets may serve as predictive biomarkers for relapse (Patterson and Copland 2023). In this study, we emphasized for the first time the role of iNKT^{+}CD161^{+} cells in TFR. The mechanism of action is linked to their cytotoxic activity and ability to modulate the anti-tumor response by activating other immune cells. Studies have indicated that there is a correlation between the functional capacity of iNKT and innate CD8^{+} T cells, suggesting their coordination in the anti-tumor immune response (Jacomet et al. 2017). iNKT^{+}CD161^{+} indirectly activates CD8^{+} T cells and NK cells, whose elevated percentages have been established as functional predictive markers for effective TFR in CML (Hermans et al. 2003). Activation of iNKT^{+}CD161^{+} leads to secretion of cytokines IFN-γ, enhancing the anti-tumor activity and activation of CD8^{+} T cells, and tumor necrosis factor α, triggering apoptosis of the remaining CML cells. Higher levels of activated CD8^{+} memory T lymphocytes are also observed in long-term remission patients, perhaps due to iNKT^{+}CD161^{+} activity and part of long-term immunity against relapsed CML (Fujii et al. 2013; Barbarin et al. 2020). Studies have shown that CML patients in the chronic phase have functional impairments of iNKT cells (Rossignol et al. 2012). These impairments are normalized in patients in complete remission following TKI or IFN-α. Considering the reversible defect in iNKT cell function in patients responding to TKI therapy in CML patients, they may also be a prognostic factor in other cancers, such as multiple myeloma, in which an acquired dysfunction of these cells has been proven in the malignant growth of myeloma cells, which DC can overcome pulsed with the ligand alpha-galactosylceramide (α-GalCer) (Dhodapkar et al. 2003). In CML patients who achieved TFR without relapses within 12 months, surface expression of PD1 on iNKT cells was decreased compared with patients with relapses and even compared with healthy controls, indicating reduced exhaustion and increased functionality (Decroos et al. 2024). This suggests that iNKT cell function may be involved in disease control, and their ability to directly lyse tumor cells and induce DC maturation further supports their role in TFR (Bassiri et al. 2014). Strategies that enhance iNKT cell function, such as IFN-α, checkpoint inhibitors, or agonists like α-GalCer, may improve TFR rates. Furthermore, modulation of CD1d expression represents a novel target for restoring iNKT cell function (Basbous et al. 2016).In this study, we also observed an association between PD1 expression on CD8^{+} lymphocytes and NK cells with a cytotoxic CD56^{dim}CD16^{+} immunophenotype and molecular recurrence of CML. This is consistent with our previous observations as well as

other investigations describing the exhausted phenotype of cytotoxic cells as an unfavorable prognostic factor for CML patients (Hughes et al. 2017; Decroos et al. 2024; Kwaśnik et al. 2024). Taken together, these results suggest a model in which durable TFR depends on a balance between protective innate-like immunity and avoidance of exhaustion among cytotoxic effector cells. iNKT^{+}CD161^{+} cells may play a crucial role in sustaining TFR via their innate cytotoxicity and capacity to orchestrate anti-leukemic responses, while the association of CD8^{+}PD1^{+} T cells with relapse aligns with established evidence of immune exhaustion, which impairs effective antigen-specific responses. Similarly, the correlation between PD1^{+} NK cells and recurrence underscores a compromised innate immunity, corroborated by studies highlighting NK-cell dysfunction as a barrier to successful TFR. Future immunotherapeutic strategies should aim to enhance innate cell function while preventing T- and NK-cell exhaustion, with the ultimate goal of improving long-term molecular remission and TFR success.

It should be noted that molecular analyses of tumor-associated gene expression were performed in a separate cohort of 43 newly diagnosed patients, whereas cytomometric analyses and *BCR::ABL1* kinetics were conducted in an independent cohort of 78 patients who discontinued TKI therapy. Due to the distinct nature of these patient groups, direct correlations between gene expression profiles and immunophenotypic or molecular remission data could not be performed. Nevertheless, both approaches provide complementary insights and offer complementary perspectives on CML biology: gene expression profiling at diagnosis highlights potentially immunogenic targets in CML, while immune profiling at TKI discontinuation identifies cellular predictors associated with sustained TFR. In a subset of three patients, additional functional assays were performed to explore cytotoxic activity against selected tumor peptides screened and newly synthesized ones derived from SPAG9 and NEWREN60. The goal of these exploratory analyses was to gain preliminary insight into the functioning of immune cells, which will allow us to understand the cellular mechanisms that could potentially sustain TFR.

Overall, our study highlights immune correlates associated with the maintenance of TFR and underscores the need for further research to clarify the mechanistic role of immune surveillance in CML. These findings underscore the need for larger studies to validate the predictive value of immune markers and explore therapeutic strategies that could enhance immune surveillance. Future research efforts should seek to validate the characterized immune markers in larger patient groups with assessment of cause-and-effect relationships and explore the efficacy of combination therapies, such as checkpoint inhibitors or LAA vaccines, in enhancing immune surveillance in CML. The incorporation of immune profiling into the clinic has the potential to transform patient management, enhancing outcomes and increasing the population of patients that can be offered successful TKI discontinuation (Irani et al. 2020; Fassoni et al. 2025).

Funding

This work was supported by the National Science Center in Poland, No. NCN 2018/31/B/NZ6/03361; to KG.

Contribution Statement

KG and TS conceived the concept of the study and contributed to the design of the research. PK, MS, KS, MaPa, AK, MiPi, PC, DLL, and MZ performed research. PK, MK, MS, MP, and KS analyzed the data. PK, MS, MaPa, JZ, KG, and TS were responsible for drafting or revising the manuscript. KG coordinated funding for the project. All authors are accountable for all aspects of the work and have approved the final version of the manuscript.

Declarations of Interest

None.

References

Abruzzese E, Trawinska MM, Coletta A et al. (2009) Peptide-vaccine treatment associated with TKI therapy in patients with CML is able to induce immunologic, cytogenetic and molecular responses: a single center experience with long-term follow up. Blood 114:2185. https://doi.org/10.1182/blood.V114.22.2185.2185

Barbarin A, Abdallah M, Lefèvre L et al. (2020) Innate T-αβ lymphocytes as new immunological components of anti-tumoral "off-target" effects of the tyrosine kinase inhibitor dasatinib. Sci Rep 10:3245. https://doi.org/10.1038/s41598-020-60195-z

Basbous S, Levescot A, Piccirilli N et al. (2016) The Rho–ROCK pathway as a new pathological mechanism of innate immune subversion in chronic myeloid leukaemia. J Pathol 240:262–268. https://doi.org/10.1002/path.4779

Bassiri H, Das R, Guan P et al. (2014) iNKT cell cytotoxic responses control T-lymphoma growth in vitro and in vivo. Cancer Immunol Res 2:59–69. https://doi.org/10.1158/2326-6066.CIR-13-0104

Benjamini Y, Hochberg Y (1995) Controlling the false discovery rate: a practical and powerful approach to multiple testing. J R Stat Soc Ser B 57:289–300. https://doi.org/10.1111/J.2517-6161.1995.tb02031.x

Bocchia M, Gentili S, Abruzzese E et al. (2005) Effect of a p210 multipeptide vaccine associated with imatinib or interferon in patients with chronic myeloid leukaemia and persistent residual disease: a multicentre observational trial. Lancet 365:657–662. https://doi.org/10.1016/s0140-6736(05)17945-8

Braga AGO, Barbosa Pagnano KB, Campioni MDP et al. (2024) Peripheral lymphocyte subsets as predicting factors for molecular recurrence after imatinib discontinuation in a phase 2 imatinib discontinuation trial in patients with chronic myeloid leukemia. Hematol Transfus Cell Ther 46:268–272. https://doi.org/10.1016/j.htct.2023.06.001

Burchert A, Saussele S, Michel C et al. (2022) Efficacy of ropeginterferon Alpha 2b in inducing treatment free remission in chronic myeloid leukemia – an International, Randomized Phase III Trial (ENDURE, CML-IX) of the German CML-Study Group. Blood 140(Suppl. 1):1501–1503. https://doi.org/10.1182/blood-2022-169324

Cathcart K, Pinilla-Ibarz J, Korontsvit T et al. (2004) A multivalent bcr-abl fusion peptide vaccination trial in patients with chronic myeloid leukemia. Blood 103:1037–1042. https://doi.org/10.1182/BLOOD-2003-03-0954

Cayssials E, Jacomet F, Piccirilli N et al. (2019) Sustained treatment-free remission in chronic myeloid leukaemia is associated with an increased frequency of innate CD8(+) T-cells. Br J Haematol 186:54–59. https://doi.org/10.1111/BJH.15858

Chang MC, Cheng HI, Hsu K et al. (2019) NKG2A down-regulation by dasatinib enhances natural killer cytotoxicity and accelerates effective treatment responses in patients with chronic myeloid leukemia. Front Immunol 9:3152. https://doi.org/10.3389/fimmu.2018.03152

Clark RE, Christmas SE (2001) BCR-ABL fusion peptides and cytotoxic T cells in chronic myeloid leukaemia. Leuk Lymphoma 42:871–880. https://doi.org/10.3109/10428190109097706

Clark RE, Dodi IA, Hill SC et al. (2001) Direct evidence that leukemic cells present HLA-associated immunogenic peptides derived from the BCR-ABL b3a2 fusion protein. Blood 98:2887–2893. https://doi.org/10.1182/blood.V98.10.2887

Collins RH Jr, Shpilberg O, Drobyski WR et al. (1997) Donor leukocyte infusions in 140 patients with relapsed malignancy after allogeneic bone marrow transplantation. J Clin Oncol 15:433–444. https://doi.org/10.1200/JCO.1997.15.2.433

Decroos A, Meddour S, Demoy M et al. (2024) The CML experience to elucidate the role of innate T-cells as effectors in the control of residual cancer cells and as potential targets for cancer therapy. Front Immunol 15:1473139. https://doi.org/10.3389/fimmu.2024.1473139

Dhodapkar MV, Geller MD, Chang DH et al. (2003) A reversible defect in natural killer T cell function characterizes the progression of premalignant to malignant multiple myeloma. J Exp Med 197:1667–1676. https://doi.org/10.1084/jem.20021650

Dou N, Hu Q, Li L et al. (2020) USP32 promotes tumorigenesis and chemoresistance in gastric carcinoma via upregulation of SMAD2. Int J Biol Sci 16:1648–1657. https://doi.org/10.7150/ijbs.43117

Fassoni AC, Yong ASM, Clark RE et al (2025) Predicting treatment-free remission in chronic myeloid leukemia patients using an integrated model of tumor-immune dynamics. npj Syst Biol Appl 2025 111 11:1–13. https://doi.org/10.1038/s41540-025-00598-8

Fujii S, Shimizu K, Okamoto Y et al. (2013) NKT cells as an ideal anti-tumor immunotherapeutic. Front Immunol 4:409. https://doi.org/10.3389/fimmu.2013.00409

Fujioka Y, Sugiyama D, Matsumura I et al. (2021) Regulatory T cell as a biomarker of treatment-free remission in patients with chronic myeloid leukemia. Cancers 13:5904. https://doi.org/10.3390/cancers13235904

Garcia CAB, Binelli LS, Palma LC et al. (2024) Immune content of mature and licensed cytotoxic cells is associated with treatment-free remission in chronic myeloid leukemia. Blood 144(Suppl. 1):1756. https://doi.org/10.1182/blood-2024-208109

Giallongo C, Parrinello N, Tibullo D et al. (2014) Myeloid derived suppressor cells (MDSCs) are increased and exert immunosuppressive activity together with polymorphonuclear leukocytes (PMNs) in chronic myeloid leukemia patients. PLoS One 9:e101848. https://doi.org/10.1371/journal.pone.0101848

Giannopoulos K, Dmoszynska A, Rolinski J et al. (2009) Identification of RHAMM-derived CD8$^+$ restricted, heteroclitical, cryptic epitope R9Y as a promising target for immunotherapy of chronic lymphocytic leukemia. Blood 114:3034. https://doi.org/10.1182/blood.v114.22.3034.3034

Greiner J, Schmitt M (2008) Leukemia-associated antigens as target structures for a specific immunotherapy in chronic myeloid leukemia. Eur J Haematol 80:461–468. https://doi.org/10.1111/J.1600-0609.2008.01053.x

Gross DA, Graff-Dubois S, Opolon P et al. (2004) High vaccination efficiency of low-affinity epitopes in antitumor immunotherapy. J Clin Invest 113:425–433. https://doi.org/10.1172/JCI19418

Guglielmi C, Arcese W, Dazzi F et al. (2002) Donor lymphocyte infusion for relapsed chronic myelogenous leukemia: prognostic relevance of the initial cell dose. Blood 100:397–405. https://doi.org/10.1182/blood.v100.2.397

Hermans IF, Silk JD, Gileadi U et al. (2003) NKT cells enhance CD4$^+$ and CD8$^+$ T cell responses to soluble antigen in vivo through direct interaction with dendritic cells. J Immunol 171:5140–5147. https://doi.org/10.4049/jimmunol.171.10.5140

Huff CA, Fuchs EJ, Smith BD et al. (2006) Graft-versus-host reactions and the effectiveness of donor lymphocyte infusions. Biol Blood Marrow Transplant 12:414–421. https://doi.org/10.1016/j.bbmt.2005.11.520

Hughes A, Clarson J, Tang C et al. (2017) CML patients with deep molecular responses to TKI have restored immune effectors and decreased PD-1 and immune suppressors. Blood 129:1166–1176. https://doi.org/10.1182/blood-2016-10-745992

Hughes TP, Ross DM (2016) Moving treatment-free remission into mainstream clinical practice in CML. Blood 128:17–23. https://doi.org/10.1182/blood-2016-01-694265

Huuhtanen J, Adnan-Awad S, Theodoropoulos J et al. (2024) Single-cell analysis of immune recognition in chronic myeloid

leukemia patients following tyrosine kinase inhibitor discontinuation. Leukemia 38:109–125. https://doi.org/10.1038/s41375-023-02074-w

Hu W, Wei H, Li K et al. (2017) Downregulation of USP32 inhibits cell proliferation, migration and invasion in human small cell lung cancer. Cell Prolif 50:e12343. https://doi.org/10.1111/cpr.12343

Ilander M, Olsson-Strömberg U, Schlums H et al. (2017) Increased proportion of mature NK cells is associated with successful imatinib discontinuation in chronic myeloid leukemia. Leukemia 31:1108–1116. https://doi.org/10.1038/leu.2016.360

Irani YD, Hughes A, Clarson J et al. (2020) Successful treatment-free remission in chronic myeloid leukaemia and its association with reduced immune suppressors and increased natural killer cells. Br J Haematol 191:433–441. https://doi.org/10.1111/bjh.16718

Jacomet F, Cayssials E, Barbarin A et al. (2017) The hypothesis of the human iNKT/Innate CD8(+) T-cell axis applied to cancer: evidence for a deficiency in chronic myeloid leukemia. Front Immunol 7:688. https://doi.org/10.3389/fimmu.2016.00688

Kanojia D, Garg M, Saini S et al. (2010) Sperm associated antigen 9 expression and humoral response in chronic myeloid leukemia. Leuk Res 4:858–863. https://doi.org/10.1016/j.leukres.2010.01.017

Kjaer L, Skov V, Andersen MT et al. (2019) Variant-specific discrepancy when quantitating BCR-ABL1 e13a2 and e14a2 transcripts using the Europe against cancer qPCR assay. Eur J Haematol 103:26–34. https://doi.org/10.1111/ejh.13238

Kolb HJ, Schattenberg A, Goldman JM et al. (1995) Graft-versus-leukemia effect of donor lymphocyte transfusions in marrow grafted patients. Blood 86:2041–2050. https://doi.org/10.1182/blood.v86.5.2041.bloodjournal8652041

Kong J, Qin YZ, Zhao XS et al. (2021) Profiles of NK cell subsets are associated with successful tyrosine kinase inhibitor discontinuation in chronic myeloid leukemia and changes following interferon treatment. Ann Hematol 100:2557–2566. https://doi.org/10.1007/S00277-021-04606-9

Kreutzman A, Yadav B, Brummendorf TH et al. (2019) Immunological monitoring of newly diagnosed CML patients treated with bosutinib or imatinib first-line. Oncoimmunology 8:e1638210 (13 pages). https://doi.org/10.1080/2162402X.2019.1638210

Kwaśnik P, Giannopoulos K (2021) Treatment-free remission-a new aim in the treatment of chronic myeloid leukemia. J Pers Med 11:697. https://doi.org/10.3390/jpm11080697

Kwaśnik P, Zaleska J, Link-Lenczowska D et al. (2024) High level of $CD8^{+}PD\text{-}1^{+}$ cells in patients with chronic myeloid leukemia who experienced loss of MMR after imatinib discontinuation. Cells 13:723. https://doi.org/10.3390/CELLS13080723

Larsen MV, Lundegaard C, Lamberth K et al. (2007) Large-scale validation of methods for cytotoxic T-lymphocyte epitope prediction. BMC Bioinformatics 8:424. https://doi.org/10.1186/1471-2105-8-424

Li S, Yang L, Ding X et al. (2024) USP32 facilitates non-small cell lung cancer progression via deubiquitinating BAG3 and activating RAF-MEK-ERK signaling pathway. Oncogenesis 13:27. https://doi.org/10.1038/s41389-024-00528-z

Li Y, Lin C, Schmidt CA (2012) New insights into antigen specific immunotherapy for chronic myeloid leukemia. Cancer Cell Int 12:52. https://doi.org/10.1186/1475-2867-12-52

Liu C, Lu X, Fang H et al. (2024) Leukemia associated macrophages and neutrophils contribute to immune suppression through PD-L1 and arginase in BCR-ABL1 chronic myeloid leukemia. Blood 144(Supl 1):6573. https://doi.org/10.1182/blood-2024-208465

Mahon FX, Réa D, Guilhot J et al. (2010) Discontinuation of imatinib in patients with chronic myeloid leukaemia who have maintained complete molecular remission for at least 2 years: the prospective, multicentre Stop Imatinib (STIM) trial. Lancet Oncol 11:1029–1035. https://doi.org/10.1016/S1470-2045(10)70233-3

Martínez-López J, Mustjoki S, Porkka K et al. (2021) The safety and efficacy of dasatinib plus nivolumab in patients with previously treated chronic myeloid leukemia: results from a phase 1b dose-escalation study. Leuk Lymphoma 62:2040–2043. https://doi.org/10.1080/10428194.2021.1889536

Maurer K, Antin JH (2024) The graft versus leukemia effect: donor lymphocyte infusions and cellular therapy. Front Immunol 15:1328858. https://doi.org/10.3389/fimmu.2024.1328858

Mori S, Vagge E, le Coutre P et al. (2015) Age and dPCR can predict relapse in CML patients who discontinued imatinib: the ISAV study. Am J Hematol 90:910–914. https://doi.org/10.1002/ajh.24120

Mumprecht S, Schürch C, Schwaller J et al. (2009) Programmed death 1 signaling on chronic myeloid leukemia-specific T cells results in T-cell exhaustion and disease progression. Blood 114:1528–1536. https://doi.org/10.1182/blood-2008-09-179697

Mustjoki S, Ekblom M, Arstila TP et al. (2009) Clonal expansion of T/NK-cells during tyrosine kinase inhibitor dasatinib therapy. Leukemia 23:1398–1405. https://doi.org/10.1038/leu.2009.46

Najima Y, Yoshida C, Iriyama N et al. (2018) Regulatory T cell inhibition by dasatinib is associated with natural killer cell differentiation and a favorable molecular response—the final results of the D-first study. Leuk Res 66:66–72. https://doi.org/10.1016/j.leukres.2018.01.010

Narita M, Masuko M, Kurasaki T et al. (2010) WT1 peptide vaccination in combination with imatinib therapy for a patient with CML in the chronic phase. Int J Med Sci 7:72–81. https://doi.org/10.7150/ijms.7.72

Nicolini FE, Dulucq S, Guilhot J et al. (2018) The evaluation of residual disease by digital PCR, and TKI duration are critical predictive factors for molecular recurrence after for stopping imatinib first-line in chronic phase CML patients: results of the STIM2 Study. Blood 132(Suppl. 1):462. https://doi.org/10.1182/blood-2018-99-113029

Oji Y, Oka Y, Nishida S et al. (2010) WT1 peptide vaccine induces reduction in minimal residual disease in an imatinib-treated CML patient. Eur J Haematol 85:358–360. https://doi.org/10.1111/j.1600-0609.2010.01497.x

Pan J, Yu H, Guo Z et al. (2018) Emerging role of sperm-associated antigen 9 in tumorigenesis. Biomed Pharmacother 103:1212–1216. https://doi.org/10.1016/j.biopha.2018.04.168

Patterson SD, Copland M (2023) The bone marrow immune microenvironment in CML: treatment responses, treatment-free remission, and therapeutic vulnerabilities. Curr Hematol Malig Rep 18:19–32. https://doi.org/10.1007/s11899-023-00688-6

Qazilbash MH, Wieder E, Thall PF et al. (2017) PR1 peptide vaccine induces specific immunity with clinical responses in myeloid malignancies. Leukemia 31:697–704. https://doi.org/10.1038/LEU.2016.254

Rammensee H, Bachmann J, Emmerich NP et al. (1999) SYFPEITHI: database for MHC ligands and peptide motifs. Immunogenetics 50:213–219. https://doi.org/10.1007/s002510050595

Rea D, Henry G, Khaznadar Z et al. (2017) Natural killer-cell counts are associated with molecular relapse-free survival after imatinib discontinuation in chronic myeloid leukemia: the IMMUNOSTIM study. Haematologica 102:1368–1377. https://doi.org/10.3324/haematol.2017.165001

Rezvani K, Grube M, Brenchley JM et al. (2003) Functional leukemia-associated antigen-specific memory $CD8^+$ T cells exist in healthy individuals and in patients with chronic myelogenous leukemia before and after stem cell transplantation. Blood 102:2892–2900. https://doi.org/10.1182/blood-2003-01-0150

Rezvani K, Yong AS, Mielke S et al. (2008) Leukemia-associated antigen-specific T-cell responses following combined PR1 and WT1 peptide vaccination in patients with myeloid malignancies. Blood 111:236–242. https://doi.org/10.1182/BLOOD-2007-08-108241

Rojas JM, Knight K, Wang L et al. (2007) Clinical evaluation of BCR-ABL peptide immunisation in chronic myeloid leukaemia: results of the EPIC study. Leukemia 21:2287–2295. https://doi.org/10.1038/sj.leu.2404858

Ross DM, Branford S, Seymour JF et al. (2013) Safety and efficacy of imatinib cessation for CML patients with stable undetectable minimal residual disease: results from the TWISTER study. Blood 122:515–522. https://doi.org/10.1182/blood-2013-02-483750

Rossignol A, Levescot A, Jacomet F et al. (2012) Evidence for BCR-ABL-dependent dysfunctions of iNKT cells from chronic myeloid leukemia patients. Eur J Immunol 42:1870–1875. https://doi.org/10.1002/eji.201142043

Saussele S, Richter J, Guilhot J et al. (2018) Discontinuation of tyrosine kinase inhibitor therapy in chronic myeloid leukaemia (EURO-SKI): a prespecified interim analysis of a prospective, multicentre, non-randomised, trial. Lancet Oncol 19:747–757. https://doi.org/10.1016/S1470-2045(18)30192-x

Sehn LH, Alyea EP, Weller E et al. (1999) Comparative outcomes of T-cell-depleted and non-T-cell-depleted allogeneic bone marrow transplantation for chronic myelogenous leukemia: impact of donor lymphocyte infusion. J Clin Oncol 17:561–568. https://doi.org/10.1200/JCO.1999.17.2.561

Sicuranza A, Breccia M, Iuliano F et al. (2025) Therapeutic vaccinations with p210 peptides in imatinib-treated chronic myeloid leukemia patients: 10 years follow-up of GIMEMA CML0206 and SI0207 studies. Vaccines (Basel) 13:419. https://doi.org/10.3390/vaccines13040419

Šmahel M (2011) Antigens in chronic myeloid leukemia: implications for vaccine development. Cancer Immunol Immunother 60:1655–1668. https://doi.org/10.1007/S00262-011-1126-z

Suwabe T, Shibasaki Y, Tamura S et al. (2024) Decade-long WT1-specific CTLs induced by WT1 peptide vaccination. Int J Hematol 119:399–406. https://doi.org/10.1007/S12185-024-03723-1

Takahashi M (2015) Long-term molecular remission with an increase of WT1-specific CTLs after cessation of WT1 peptide vaccination in a patient with CML. Ann Oncol 26(Suppl. 2):ii23. https://doi.org/10.1093/annonc/mdv093.4

Tanaka A, Nishikawa H, Noguchi S et al. (2020) Tyrosine kinase inhibitor imatinib augments tumor immunity by depleting effector regulatory T cells. J Exp Med 217:e20191009. https://doi.org/10.1084/JEM.20191009

van Rhee F, Lin F, Cullis JO et al. (1994) Relapse of chronic myeloid leukemia after allogeneic bone marrow transplant: the case for giving donor leukocyte transfusions before the onset of hematologic relapse. Blood 83:3377–3383. https://doi.org/10.1182/blood.v83.11.3377.3377

Vigón L, Rodríguez-Mora S, Luna A et al. (2020) Cytotoxic cell populations developed during treatment with tyrosine kinase inhibitors protect autologous $CD4^+$ T cells from HIV-1 infection. Biochem Pharmacol 182:114203. https://doi.org/10.1016/j.bcp.2020.114203

Vita R, Mahajan S, Overton JA et al. (2019) The Immune Epitope Database (IEDB): 2018 update. Nucleic Acids Res 47:D339–D343. https://doi.org/10.1093/nar/gky1006

Webster JA, Robinson TM, Blackford AL et al. (2021) A randomized, phase II trial of adjuvant immunotherapy with durable TKI-free survival in patients with chronic phase CML. Leuk Res 111:106737. https://doi.org/10.1016/j.leukres.2021.106737

Xiu M, Bao W, Wang J et al. (2023) High USP32 expression contributes to cancer progression and is correlated with immune infiltrates in hepatocellular carcinoma. BMC Cancer 23:1105. https://doi.org/10.1186/s12885-023-11617-4

Yong AS, Keyvanfar K, Eniafe R et al. (2008) Hematopoietic stem cells and progenitors of chronic myeloid leukemia express leukemia-associated antigens: implications for the graft-versus-leukemia effect and peptide vaccine-based immunotherapy. Leukemia 22:1721–1727. https://doi.org/10.1038/leu.2008.161

74, 4 (2026), DOI: 10.2478/aite-2026-0004

Supplementary Figures

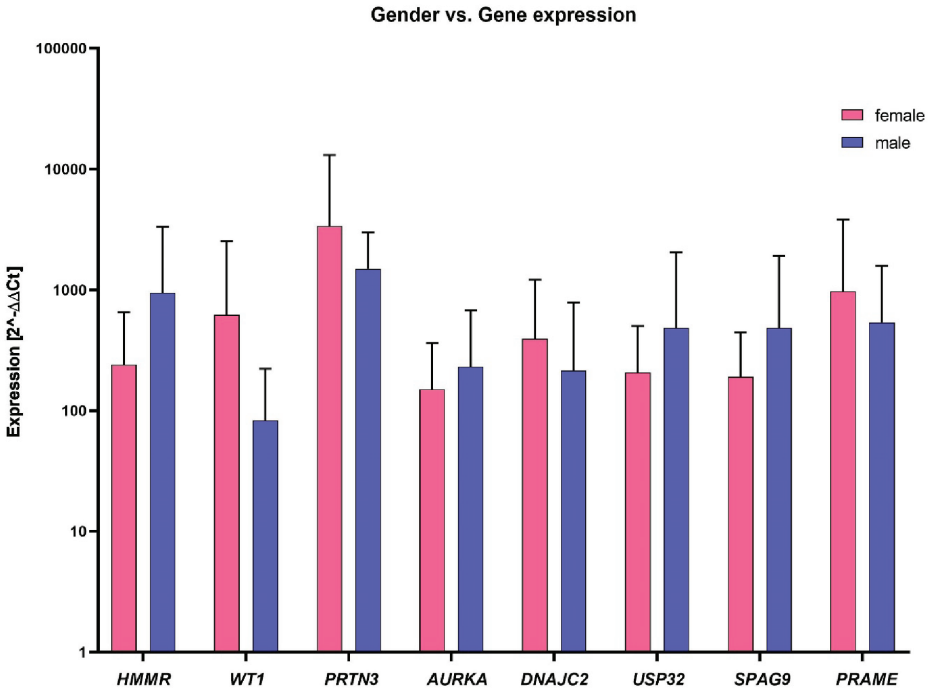

Fig 1. *Evaluation of the correlation between analyzed genes and the gender of the CML patients. Results, shown as mean with SD, were obtained by performing Mann-Whitney non-parametric test. There was no statistically significant correlation between the expression of each of the analyzed genes and the gender of the CML patients.*

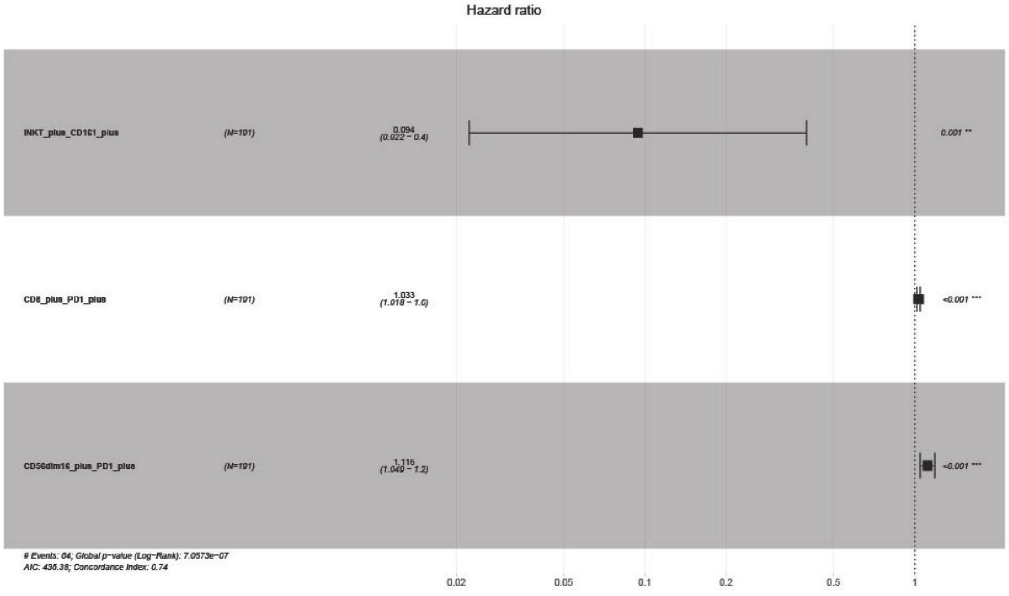

Fig 2. *Forest plot of the Cox proportional hazards model for immune cell markers. The forest plot illustrates the hazard ratios (HR) and 95% confidence intervals (CI) for immune cell markers included in the Cox proportional hazards model. Each marker is represented by a point estimate for the HR and a horizontal line indicating its 95% confidence interval. The vertical dashed line at HR = 1 represents the threshold for no effect. Markers positioned entirely to the left of this line suggest a protective effect, while those to the right indicate an increased risk. The number of observations (N) and the number of events are also indicated. A global p-value from the log-rank test confirms the overall model significance. Additionally, the Akaike Information Criterion (AIC) and Concordance Index (C-index) reflect the model's goodness-of-fit and predictive accuracy.*

74, 4 (2026), DOI: 10.2478/aite-2026-0004

Supplementary Tables

Table 1. *Correlation between patients age and expression of the analyzed genes.*

Analyzed gene	*HMMR*	*WT1*	*PRTN3*	*AURKA*	*DNAJC2*	*USP32*	*SPAG9*	*PRAME*
r	0.1019	-0.0712	-0.0888	-0.0792	0.1098	0.2229	0.0955	-0.0251
p	0.5206	0.6625	0.5760	0.6179	0.4888	0.1668	0.5527	0.8812

Results were obtained by performing Spearman rank correlation test. There was no statistically significant correlation between the expression of each of the analyzed genes and the age of the CML patients.

Table 2. *Univariate Summary*

Univariate Model	Hazard Ratio (95% CI)	P-value
CD4_plus_CD25_plus_FoxP3_plus.txt	0.89 (0.77 – 1.01)	0.077
CD56dim16_plus_PD1_plus.txt	1.06 (1.01 – 1.11)	0.024
CD8_plus_PD1_plus.txt	1.03 (1.02 – 1.05)	< 0.001
iNKT_plus_CD161_plus.txt	0.32 (0.11 – 0.94)	0.039
Model Comparison_Metrics		
Model	AIC	Concordance
CD8_plus_PD1_plus.txt	467.8898	0.6512
iNKT_plus_CD161_plus.txt	477.1068	0.5927
CD56dim16_plus_PD1_plus.txt	478.4037	0.5312
CD4_plus_CD25_plus_FoxP3_plus.txt	479.6236	0.5984

Table 3. *Model_Comparison*

Model	AIC	Concordance
cox_model_summary_stepwise_model	430.0106	0.7923
cox_model_summary_model_01	433.9947	0.7621
cox_model_summary_model_02	436.375	0.7352
cox_model_summary_final_model	440.9907	0.7478
cox_model_summary_full_model	446.2834	0.817
cox_model_summary_model_03	448.5368	0.6547
cox_model_summary_final_model		
Characteristic	Hazard Ratio (95% CI)	P-value
iNKT_plus_CD161_plus	0.24 (0.08 – 0.73)	0.013
CD4_plus_CD25_plus_FoxP3_plus	0.87 (0.75 – 1.00)	0.049
CD8_plus_PD1_plus	1.04 (1.02 – 1.05)	< 0.001
cox_model_summary_full_model		
Characteristic	Hazard Ratio (95% CI)	P-value
DC	0.83 (5.50 – 1.27)	0.394
cDC	4.85 (3.38 – 69.52)	0.245
pDC	0.25 (4.71 – 13.67)	0.5
cDC_PD1_plus	0.96 (9.18 – 1.00)	0.076
pDC_PD1_plus	1.04 (9.95 – 1.08)	0.086
CD56dimCD16_plus	1.05 (9.69 – 1.13)	0.254
CD56brightCD16_minus	0.58 (1.69 – 2.00)	0.391
CD56brightCD16_plus	0.96 (4.83 – 1.89)	0.895

(*Continued*)

Table 3. Continued

iNKT	2.71 (6.05 – 121.03)	0.608
iNKT_plus_CD161_plus	0.01 (4.82 – 2.14)	0.093
NKT	1.04 (9.69 – 1.12)	0.265
CD56dim16_plus_PD1_plus	1.15 (1.05 – 1.26)	0.004
CD56bright16_minus_PD1_plus	0.96 (8.51 – 1.09)	0.526
iNKT_plus_PD1_plus	0.98 (9.65 – 1.00)	0.138
NKT_PD1_plus	0.97 (9.31 – 1.01)	0.102
CD4_plus	1.04 (1.00 – 1.09)	0.045
CD4_plus_PD1_plus	1.03 (9.84 – 1.08)	0.208
CD8_plus	1.08 (1.01 – 1.14)	0.013
CD8_plus_PD1_plus	1.05 (1.02 – 1.07)	< 0.001
CD19_plus	1.10 (1.03 – 1.18)	0.006
CD19_plus_PD1_plus	1.01 (9.85 – 1.03)	0.446
CD4_plus_CD25_plus_FoxP3_plus	0.75 (6.27 – 0.90)	0.002
cox_model_summary_model_01		
Characteristic	Hazard Ratio (95% CI)	P-value
iNKT_plus_CD161_plus	0.10 (0.03 – 0.40)	0.001
CD4_plus_CD25_plus_FoxP3_plus	0.86 (0.75 – 1.00)	0.05
CD8_plus_PD1_plus	1.03 (1.02 – 1.05)	< 0.001
CD56dim16_plus_PD1_plus	1.11 (1.05 – 1.18)	< 0.001
cox_model_summary_model_02		
Characteristic	Hazard Ratio (95% CI)	P-value
iNKT_plus_CD161_plus	0.09 (0.02 – 0.40)	0.001
CD8_plus_PD1_plus	1.03 (1.02 – 1.05)	< 0.001
CD56dim16_plus_PD1_plus	1.12 (1.05 – 1.19)	< 0.001
cox_model_summary_model_03		
Characteristic	Hazard Ratio (95% CI)	P-value
CD8_plus_PD1_plus	1.03 (1.02 – 1.05)	< 0.001
CD56dim16_plus_PD1_plus	1.05 (0.99 – 1.10)	0.089
cox_model_summary_stepwise_model		
Characteristic	Hazard Ratio (95% CI)	P-value
cDC_PD1_plus	0.96 (0.92 – 1.00)	0.044
pDC_PD1_plus	1.04 (1.00 – 1.08)	0.061
iNKT_plus_CD161_plus	0.08 (0.02 – 0.34)	< 0.001
CD56dim16_plus_PD1_plus	1.08 (1.02 – 1.15)	0.013
CD4_plus	1.03 (1.00 – 1.06)	0.035
CD8_plus	1.06 (1.02 – 1.11)	0.003
CD8_plus_PD1_plus	1.04 (1.02 – 1.06)	< 0.001
CD19_plus	1.07 (1.01 – 1.12)	0.012
CD4_plus_CD25_plus_FoxP3_plus	0.79 (0.67 – 0.93)	0.004